EFFECTIVE UTILIZATION OF COAL ASH FOR HIGH THERMAL SHOCK RESISTANCE GLASS-CERAMICS WARE

Waraporn Emem

A Thesis Submitted in Partial Fulfillment of the Requirement for the Degree of Master of Engineering in Ceramic Engineering

Suranaree University of Technology

Acadimic Year 2005

ISBN 974-533-539-8

การนำขี้เถ้าจากถ่านหินมาใช้อย่างมีประสิทธิผลสำหรับภาชนะกลาสเซรามิก ซึ่งทนต่อการเปลี่ยนแปลงอุณหภูมิแบบเฉียบพลันได้สูง

นางวราภรณ์ เอ็มเอ็ม

วิทยานิพนธ์นี้เป็นส่วนหนึ่งของการศึกษาตามหลักสูตรปริญญาวิศวกรรมศาสตรมหาบัณฑิต

สาขาวิชาวิศวกรรมเซรามิก

มหาวิทยาลัยเทคโนโลยีสุรนารี

ปีการศึกษา 2548

ISBN 974-533-539-8

EFFECTIVE UTILIZATION OF COAL ASH FOR HIGH THERMAL SHOCK RESISTANCE GLASS-CERAMICS WARE

Suranaree University of Technology has approved this thesis submitted in partial fulfillment of the requirements for a Master's Degree.

Thesis Examining Committee

(Dr. Veerayuth Lorprayoon)

Chairperson

(Asst. Prof. Dr. Shigeki Morimoto)

Member (Thesis Advisor)

(Assoc. Prof. Dr. Charussri Lorprayoon)

Member

(Assoc. Prof. Dr. Sutin Kuharuangrong)

Member

(Dr. Sutham Srilomsak)

Member

(Assoc. Prof. Dr. Saowanee Rattanaphani)

Vice Rector for Academic Affairs

(Assoc. Prof. Dr. Vorapot Khompis)

Dean of Institute of Engineering

วราภรณ์ เอ็มเอ็ม : การนำขี้เถ้าจากถ่านหินมาใช้อย่างมีประสิทธิผลสำหรับภาชนะกลาสเซรามิกซึ่งทนต่อการเปลี่ยนแปลงอุณหภูมิแบบเฉียบพลันได้สูง(EFFECTIVE UTILIZATION OF COAL ASH FOR HIGH THERMAL SHOCK RESISTANCE GLASS-CERAMICS WARE) อ. ที่ปรึกษา : ผศ.ดร. ชิเกกิ โมริโมโต , 95 หน้า , ISBN 974-533-539-8

การศึกษาถึงความเป็นไปได้ในการนำขี้เถ้าลอยจากการเผาถ่านหินที่โรงไฟฟ้าระยองมาใช้อย่างมีประสิทธิผลซึ่งจะใช้เป็นวัตถุดิบตัวหนึ่งสำหรับการสังเคราะห์ผลึก วอลาสโตไนท์ ในกลาสเซรามิก ใช้ขี้เถ้าลอยเป็นวัตถุดิบได้ 35 % ในส่วนผสมแก้ว แก้วที่ได้จะมีสีเขียวอมดำไม่มีฟองในเนื้อ แก้วที่ไม่มีส่วนผสมของ แคลเซียมฟลูออไรด์และสปอดูมีนหลังจากนำไปตกผลึกจะได้เฉพาะผลึกที่ผิวเท่านั้น ส่วนแก้วที่มีส่วนผสมของแคลเซียมฟลูออไรด์และสปอดูมีนจะสามารถตกผลึกได้ทั้งก้อน ชนิดของผลึกในแก้วที่มีแต่แคลเซียมฟลูออไรด์ เป็นผลึก วอลาสโตไนท์ ส่วนแก้วที่มีแคลเซียมฟลูออไรด์และสปอดูมีนจะเป็นผลึก วอลาสโตไนท์และสปอดูมีน

ในกรณีที่มีแคลเซียมฟลูออไรด์ 3% และ สปอดูมีน 20 % เป็นส่วนผสม ใช้อุณหภูมิการเกิดนิวเคลียส 750 องศาเซลเซียส เป็นเวลา 10 ชั่วโมงและตามด้วยอุณหภูมิการตกผลึก 950 องศาเซลเซียสเป็นเวลา 5 ชั่วโมง แก้วจะตกผลึกได้ 53.9% ในเนื้อ ความแข็งแรงของกลาสเซรามิก 230 $\pm$ 39 เมกกะปาสคาล ซึ่งมีความแข็งแรงมากกว่าแก้ว 2 เท่า แต่จากการตกผลึกเป็นกลาสเซรามิกค่าสัมประสิทธิ์การขยายตัวเนื่องจากความร้อนไม่แตกต่างจากแก้ว ดังนั้นการทนทานต่อการเปลี่ยนแปลงอุณหภูมิแบบเฉียบพลันของกลาสเซรามิกจะสูงกว่าแก้ว 2 เท่า

ดังนั้นการใช้ขี้เถ้าลอยจากการเผาไหม้ถ่านหินของโรงไฟฟ้าสามารถนำมาใช้เป็นวัตถุดิบสำหรับอุตสาหกรรมแก้วได้

สาขาวิชา <u>วิศวกรรมเซรามิก</u>

ปีการศึกษา 2548

ลายมือชื่อนักศึกษา _____

ลายมือชื่ออาจารย์ที่ปรึกษา _____

ลายมือชื่ออาจารย์ที่ปรึกษาร่วม _____

WARAPORN EMEM : EFFECTIVE UTILIZATION OF COAL ASH FOR HIGH THERMAL SHOCK RESISTANCE GLASS-CERAMICS WARE. THESIS ADVISOR : ASST. PROF. SHIGEKI MORIMOTO, Ph.D. 95 PP. ISBN 974-533-539-8

COAL ASH/THERMAL SHOCK RESISTANCE/GLASS-CERAMICS

The possibility of effective utilization of fly ash originating coal burning Rayong thermal power plant was investigated as one of the starting materials to synthesize wollastonite based glass-ceramics. About 35% of fly ash can be introduced into batch, and bubble free and dark green glasses were obtained. The glass free from CaF_2 or spodumene showed surface crystallization by naked eye, however, glasses containing CaF_2 and/or spodumene exhibited bulk crystallization. The crystalline phases were wollastonite for glass with CaF_2, and wollastonite and spodumene for glass with CaF_2 and spodumene. The glass with 3% CaF_2 and 20% Spodumene was used 750°C 10 hour for nucleation and 950 °C 5 hour for crystallization. The percent crystallinity was 53.9%. The fracture strength of glass-ceramics was 230$\pm$39 MPa , which was two times higher than that of glasses, and surface hardness were high. However, the thermal expansion coefficient did not change by the crystallization, and hence the thermal shock resistance was just two times higher than that of glass. Thus, the fly ash can be used for glass industry as raw material.

School of Ceramic Engineering

Academic Year 2005

Student's Signature Waraporn Emem

Advisor's Signature S. Morimoto

Co-advisor's Signature

ACKNOWLEDGEMENTS

The author wishes to acknowledge the funding support from Suranaree University of Technology (SUT).

The greatful thanks and appreciation are given to the thesis advisor, Assistant Professor Dr. Shigeki Morimoto, for his consistent supervision, advice and support throughout this project. Special thanks are also extended to Dr. Veerayuth Lorprayoon co-advisor and Associate Professor Dr. Charussri Lorprayoon for their valuable suggestion and discussion.

The author is also greatful to all the faculty and staff members of the School of Ceramic Engineering and colleagues for their help and assistance throughout the period of this study.

Finally, I thank my father, mother and family who support and encourage me during my study at Suranaree University of Technology.

Waraporn Emem

TABLE OF CONTENTS

PAGE

TABLE OF CONTENTS(continued)

PAGE

TABLE OF CONTENTS(continued)

PAGE

TABLE OF CONTENTS(continued)

PAGE

LIST OF TABLES

TABLE **PAGE**

LIST OF FIGURES

FIGURE **PAGE**

LIST OF FIGURES(continued)

FIGURE **PAGE**

LIST OF FIGURES(continued)

FIGURE **PAGE**

CHAPTER I

INTRODUCTION

The amount of incineration ash, hereafter “coal ash”, discharged from coal fired power plant increases year by year in accordance with an increasing electricity demand in the country, and this incineration ash waste causes both environmental and ecological problems.

Many applications or utilization and researches on the effective utilization of coal ashes have been done, such as a raw material for cement industry [Erol,M.Demirler,U.,Kucukbayrak,S.,Ersoy,A., and Ovecoglu,M.L.(2003)], brick and tile fabrication [Ferreira,C., Ribeiro,A., and Ottosen,L.(2003)], land filling [Cheng, T.W., and Chen,Y.S.(2003)], a filler in plastics and paint [Kutuarni,S.M., and Kishore.(2002)] and a waste treatment [Kastner,J.R., Das,K.C., and Melear,N.D. (2002)]. However, the effective crucial and economical application has not been found yet. In these circumstances, the effective utilization of coal ashes is strongly desired from environmental, ecological and economical points of view.

In recent years, many research and development investigations have been conducted in the utilization of fly ash as a starting material for glass-ceramics production. Because the chemical composition of fly ash contains large amount of SiO_2 and Al_2O_3, which are main glass network formers and a significant amount of metal oxides which are able to act as nucleating agents for nucleation and crystallization. Furthermore, fly ash is much more convenient to use than blast

furnace and steel slags. It is available in the fine powder form , which make it easier for mixing with other ingredients in a batch and in greater quantities than slag.

Glass-ceramics are polycrystalline materials produced by controlled crystallization of suitable glasses during specific heat treatment procedures. The glass-ceramic production process comprises of the preparation of a homogeneous glass, the shaping of the glass to produce the required articles and finally the application of a controlled heat treatment process. Controlled heat treatment consists of two steps; nucleation and crystal growth. In the nucleation process, the temperature is held for a sufficient time for stable nuclei formation. Following nucleation, the glass is heated to a higher temperature for a selected period of time, where the crystal growth was occurred.

One of the significant characteristics of glass-ceramics is the higher practical strength than that of glass [Benavidez,E., Grasselli,C., and Quaranta,N.(2003)]. Therefore, the problem remaining is an achievement of the lower thermal expansion coefficient. Generally, the thermal expansion coefficient of glass-ceramics based on Na_2O-MgO-CaO-Al_2O_3-SiO_2 system is relatively high, α = 70~90 x 10^{-7}/K [Barbeiri,L., Lancellotti,I., Manfredi,T., and Pellacani,G.C.(2001)]. It is well known that spodumene exhibits low thermal expansion coefficient [Wesche,K.(1991)], [Vassilev,S.V., and Vassileva,C.G. (1996)]. It is expected that the introduction of spodumene into this system may produce the lower thermal expansion coefficient glass-ceramics. Furthermore, the introduction of spodumene can also improve the chemical durability of glass-ceramics. And it is interesting that fine grained glass-ceramic can be obtained without nucleating agents from scientific and technological point of view.

1.1 Research Objective

The thermal shock resistance of brittle materials, such as ceramics and glasses, may be expressed by basic equation for extreme temperature change, for example water quenching. [Beall,G.H., and Duke,D.A.(1980)].

$$\sigma = E \cdot \alpha \cdot \Delta T / (1-\mu) \tag{1.1}$$

Where E, α, ΔT, μ and σ are Young's modulus, thermal expansion coefficient, temperature difference, Poisson's ratio, and the stress arisen by extreme temperature change, respectively. If the stress arisen exceeds the practical strength of materials, the material may be destroyed. It is clear that the higher thermal shock resistance of materials can be achieved by the higher practical strength and the lower thermal expansion coefficient according to above equation.

The objectives of the present study will be following as;

1. Preparation of high thermal shock resistant glass-ceramics ware using coal ash
2. Investigation of glass-ceramics properties for
   - High strength
   - Low coefficient of thermal expansion
   - High chemical resistance

1.2 Scope and Limitation of Study

Investigations will be carried out as follows:

1. Characterization of coal ash

2. Characterization of glass and glass-ceramics

3. Identification of type and properties of crystals

4. Evaluation of heat treatment conditions and properties of glass-ceramics.

1.3 Expected Results

1. Effective utilization of coal ash for high thermal shock resistant glass-ceramics ware.

2. Establishment of basic technology of glass-ceramics production, i.e., to design of composition and heat treatment schedule.

CHAPTER II

LITERATURE REVIEW

2.1 Coal ash

The coal ash can be classified into fly ash and bottom ash components by the location and methods of recovery[Locsei,B.P.(1964)]. An about 80% of coal ash is entrained in combustion gas, and is captured and recovered as a fly ash. The remaining 20% of ash is the bottom ash, which is collected by a water filled hopper at the bottom of the furnace of the plant.

They are basically composed of silica (SiO_2), alumina (Al_2O_3), iron oxides ($FeO+Fe_2O_3$), alkali and alkaline earth oxides with a small amount of various heavy metal and transition metal oxides[Barbieri,L.,Corradi,A., and Lancellatti,I. (2000)]. The majority of fly ash is classified into two groups depending on the type of raw coals [Erol,M., Genc,A., Ovecoglu,M.L.,Yucelen,E., Kucukbayrak,S., and Taptik,Y.(2000)];

A. Class F; normally produced by the combustion of anthracite or bituminous coal, this is aluminosilicate ash which has pozzolanic properties. (A material such as certain fly ashes and blast furnace slags which, in finely devided form will exhibit cementitious properties. When mixed with lime and water) [Loran,S.(1994)].

B. Class C; normally produced from lignite or sub-bituminous coal, this is calcium sulphate ash which has both pozzolanic and some cementitious properties.

It is well known that coal ashes mainly consist of glassy phase with a small amount of crystals [Baebieri,L., Lancellotti,I., Manfredini,T., Queralt,I., Rincon,J.M., and Romeo,M.(1999)].

2.2. Glass

Glass was described as a transparent material possessing the properties of hardness, rigidity and brittleness. Thus with the possible exception of transparency, the properties usually thought of as glass are those normally associated with solids. Various definitions of glass have been put forward but one which is widely accepted is that proposed by the A.S.T.M.: "*glass is an inorganic product of fusion which has cooled to a rigid condition without crystallizing.*"

There are many properties of glass which confirm its liquid-like nature. For example, the transparency of glass may be thought of as a property more usually characteristic of the liquid state than that of the solid crystalline state, the transparency of glass is a result of the complete absence of grain boundaries or inclusions which could cause scattering of light. The X-ray diffraction pattern of glass shows only diffuse haloes as compared with the sharp pattern of line given by a crystalline substance.

Every glass found to date shares two common characteristics; first, no glass has a long range, periodic atomic arrangement. Evenmore importantly, every glass exhibits the time-dependent behavior known as glass transformation behaviour. This behaviour occurs over a temperature range known as the glass transformation region. A glass can be defined as "an amorphous solid completely lacking in long range, periodic atomic structure and exhibiting a region of glass tranformation behavior."

The glass transformation behaviour has been discussed on the basis of either enthalpy or volume versus temperature diagrams, such as that shown in the figure 2-1

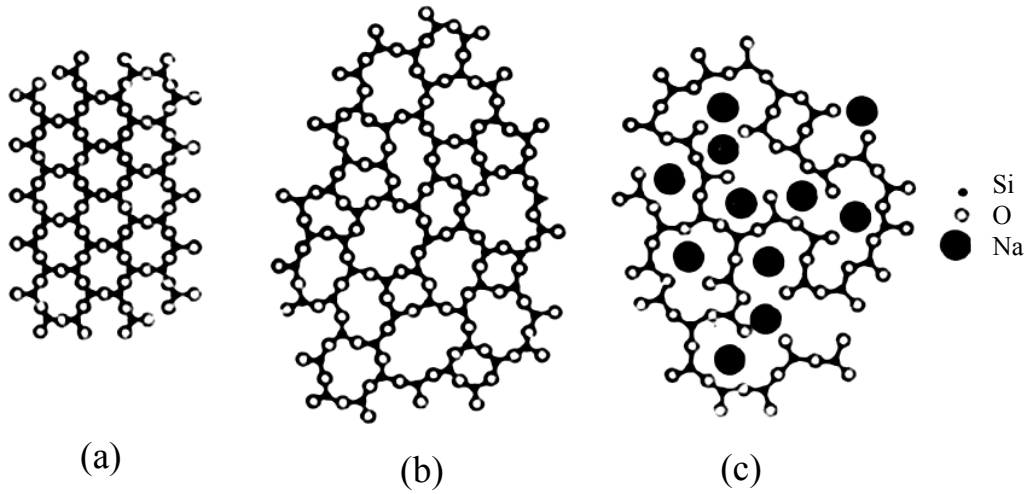

Figure 2.1 Schematic two-dimensional representation of the structure of

a) crystalline silica

b) silica glass

c) sodium silicate glass [Mcmillan,P.W.,(1964)]

If the liquid can be cooled below the melting temperature of the crystal without crystallization, a supercooled liquid is obtained. The atomic structure of the liquid continues to rearrange as the temperature decreases, but no abrupt decrease in enthalpy due to a discontinuous structure rearrangement occurs. As the liquid is cooled further, the viscosity increases, and this increase in viscosity eventually becomes so great that the atoms can no longer completely rearrange to the equilibrium liquid structure during the time allowed by the experiment. The temperature region lying between the limits where the enthalpy is that of the

equilibrium liquid and that of the frozen solid is known as the glass transformation region. The frozen liquid is now a glass.

Scientist attempted to quantify the mixed bond concept by use of the partial ionic character model of Pauling, that classified oxides into three groups on the basis of the electronegativity of the cation. Since the anion is oxygen in every case, this approach effectively identical to grouping by fractional ionic character of the cation-anion bond. Cations which form bonds with oxygen with a fractional ionic character near 50% should act as *network formers* (group I) and produce good glasses. Cations with slightly lower electronegativities (group II), which form slightly more ionic bonds with oxygen, cannot form glasses by themselves, but can partially replace cations from the first group. Since these ions behave in a manner which is intermediate between that of cations which do form glasses and those which never form glasses, they are known as *intermediates.* Finally, cations which have very low electronegativities (group III), and therefore form highly ionic bonds with oxygen, never act as network formers. Since these ions only serve to modify the network structure created by the network-forming oxides, they are termed *modifiers.*

2.3 Glass-ceramics

Glass-ceramics are microcrystalline solids produced by controlling devitrification (crystallization) of glass. Glasses are melted, fabricated to shape, and then converted to a predominantly crystalline ceramics by heat treatment. The basis of controlled crystallization lies in efficient internal nucleation, which allows development of fine, randomly oriented grains without voids, or other porosity. The

discovery of the role of nucleating agents in initiating glass crystallization from a multitude of centers was the major factor allowing the introduction of glass-ceramics.

Silicate glasses have a random structure based on an irregular arrangement of SiO_4 tetrahedra linked through corner sharing into a three-dimentional network. The difference in structure between vitreous silica and the crystalline polymorphs of silica lies primarily in long range order (beyond about 8 A^o). Both are composed structurally of the same cation-anion polyhedral with similar linkage, but the crystalline forms show continuous spatial pattern repetition; the vitreous form is random.

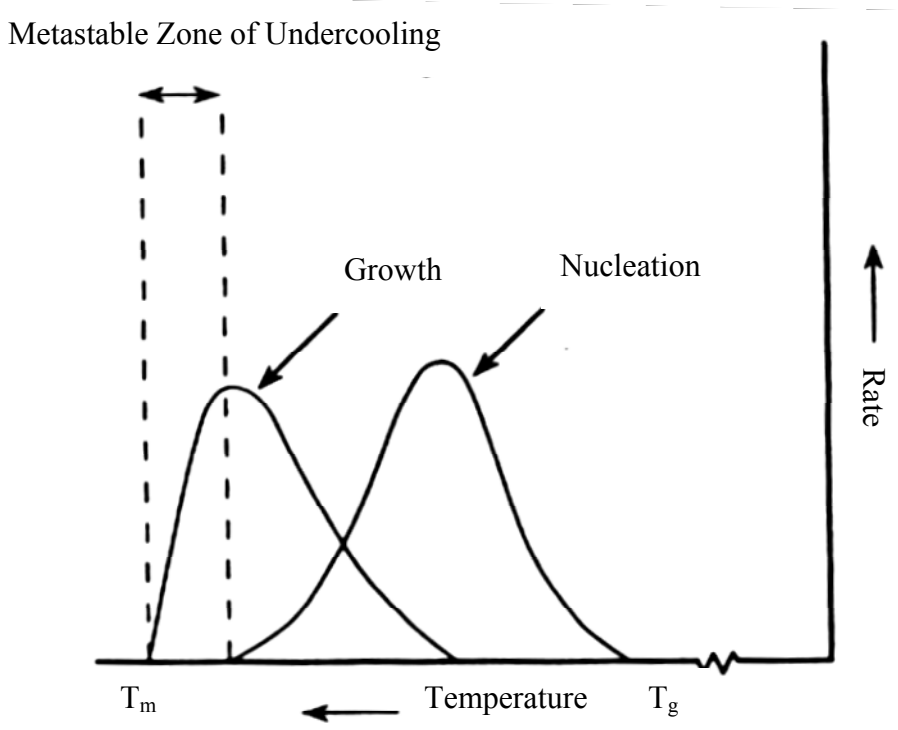

Figure 2.2 Effect of temperature on the rates of nucleation and crystal growth for a glassforming melt. [Shelby,J.E.,1997]

Cations have been classified into three groups according to their role in the structure of oxide glasses: network formers, such as Si, B, P, Ge, and As, have oxygen coordination numbers of 3 or 4 and tend to produce the basic cross-linked polymeric glass structure; network modifiers, such as Na, K, Ca, and Ba, have coordination number of 6 or more and generally tend to reduce the polymerization and viscosity of the glass and modify the properties of glass; intermediate oxides with cations such as Al, Zn, Mg, Pb, and Be have intermediate coordination number of 4 or 6 and may either act as modifier or replace network cations, depending on the glass composition.

Homogeneous and heterogeneous nucleation

A homogeneous viscous liquid is cooled below the equilibrium solubility point of the most insoluble species (liquidus temperature). It enters a metastable region in which do not form at a detectable rate but where crystals, once nucleated, can easily grow. Below this temperature region, nuclei may spontaneously and uniformly form, but with cooling, the liquid reaches a high viscosity that impedes both the formation and growth of nuclei.

1) Homogeneous nucleation and growth rates are functions of temperature for a typical undercooled liquid of high viscosity. These rates follow relations of the types,

For nucleation rate;

$$I = A \exp((-\Delta F^* + Q)/kT \qquad (2.1)$$

Where, I : Homogeneous nucleation rate

ΔF^* :The maximum free energy change at the critical radius of a spherical nucleus.

Q : Activation energy for short range diffusion of atoms or molecules across the interface

A : Constant approximately equal to $n_v kT/h'$

$$A = n_v kT/h' \tag{2.2}$$

n_v : the number of formula units of the crystallizing component phase per unit volume of the melt

k : Boltzmann constant

h': Plank constant

And for crystal growth;

$$U = f.R.T(1-\exp \Delta G/RT)3\pi.N.a_0^2 \tag{2.3}$$

U : The rate of crystal growth

f : The fraction of the total number of sites available for growth

ΔG :The bulk free energy change by crystallization

R : Gas constant

a_0 : interatomic separation

η : The viscosity of the liquid

Most glass-forming liquids, when supercooled, do not crystallize according to the basic laws of homogeneous nucleation. Nucleation usually occurs at the surface of

glass in contact with air or other foreign substances where abundant nuclei are already present. When internal crystallization does occur, it almost always results from the nucleation of the major crystalline components upon nuclei of foreign, highly insoluble particle, i.e., metallic particles halides, sulfides, and certain oxides. These forms of induced nucleation are controlled by irregularities in the glass structure or foreign particles within or on the glass surface and are referred to as heterogeneous nucleation. Most glasses, if held for a long peroid at temperatures below their liquiduses, but considerably above their annealing point, will crystallize from the surface by heterogeneous nucleation. At the surface, coordination of certain ions is incomplete and devitrification from bulk structures are locally large. This creates a high-energy state where devitrification can readily occur. An abundance of foreign nuclei doubtless enhances this phenomenon. Crystallization in this case proceeds generally toward the interior of the glass in a more or less oriented dendritic pattern. This form of heterogeneous nucleation and devitrification generally results in weak ceramic bodies, with coarse and oriented crystals usually accompanied by pits and voids.

2) Heterogeneous nucleation was first achieved using metallic nuclei precipitated throughout the body of glass. For centuries metals such as gold , copper, and silver have been used to produce colored glass for decorative purposes. Initially dissolved in the melt in the form of ions, they are reduced as the glass cools and finally precipitate as extremely fine colloid particles could be precipitated photochemically by the action of ultraviolet radiation on a glass containing a readily available source of electrons such as the cerous ion. The photosensitive reaction is

$$Au^{+}, Ag^{+} + Ce^{3+} \text{-----} > Au^{0}, Ag^{0} + Ce^{4} \quad (2.4)$$

Glass-ceramics have a number of key advantages over conventional ceramics [Leroy,C., Ferro,M.C., Montreiro., and Fernandes,M.H.V.(2001)]; i.e.

1. Flexibility and ease of forming,
2. Uniformity and reproducibility of properties
3. Ability to produce unique properties inherent in extremely fine grained crystalline materials
4. Lack of porosity
5. Economy of scale in high volume manufacturing process and etc.

There are six basic composition systems from which commercial glass-ceramics of economic importance are made:

1. Li_2O-Al_2O_3-SiO_2, glass-ceramics of very low thermal expansion coefficient
2. MgO-Al_2O_3-SiO_2, cordierite glass-ceramics of good mechanical, thermal and dielectric properties.
3. Li_2O- SiO_2, glass-ceramics with photochemical etching capability.
4. Na_2O-Al_2O_3-SiO_2, nepheline glass-ceramics with high mechanical strength from compression glazing.
5. K_2O-MgO-Al_2O_3-SiO_2-F, machinable fluormica glass-ceramics.
6. CaO-MgO-Al_2O_3-SiO_2, inexpensive glass-ceramics from natural materials and slags.

Many researches on the mechanism and production of glass-ceramics have been done, and many glass-ceramics products have been commercialized

[Beall,G.H.(1984)]. Two kinds of products produced from ***industrial wastes*** are known among these glass-ceramics. One is those produced from ***blast furnace slag***, and have been commercialized as floor-tile and interior or exterior wall cladding in Russia and Eastern Europe. This glass-ceramic product is called "***Slag Sitall***" and characterized by high chemical resistance, high hardness and relatively high strength [Karamanov,A., Tagliere,G., and Pelino,M.(1999)]. Another is the glass ceramics which can be produced from ***incineration ashes,coal ashes,*** discharged from coal-fired power plant. Many researches on the effective utilization of coal ashes still study in Italy [Romero,M., and Rincon,J.M.(1999)], Turkey [Barbieri,L., Ferrari,A.M., Lancellotti,I., and Leonelli,C.(2000)], Spain [Gorokhosky,A., and Escalante-Garcia,J.I.(2002)] and Portugal[Kingery,W.D., Bowen,H.K., and Uhlmann,D.R. (1991)] in recent years. The field of application of this glass-ceramics is mainly floor tile and wall cladding similar to "**Slag Sitall**".

These glass-ceramics are based on "Na_2O-CaO-MgO-Al_2O_3-SiO_2" system [Beall,G.H(1989)], and produced by the similar manner described above. Sometimes, glass cullet and other waste materials are used as raw materials with coal ashes [Karamanov,A., Tagliere,G., and Pelino,M.(1999), Romero,M., and Rincon,J.M. (1999), Barbieri,L., Ferrari,A.M., Lancellotti,I., and Leonelli,C.(2000), Gorokhosky,A., and Escalante-Garcia,J.I.(2002)]. Heavy metal sulfides are used as nucleating agents for "Slag Sitall" [Beall,G.H(1989)]. On the contrary, no nucleating agents are used for glass-ceramics produced from incineration ashes [Erol,M., Demirler,U.,Kucukbayrak,S.,Ersoy,A., and Ovecoglu,M.L.(2003), Romero,M., and Rincon,J.M. (1999), Barbieri,L., Ferrari,A.M., Lancellotti,I., and Leonelli,C.(2000), Gorokhosky,A., and Escalante-Garcia,J.I.(2002), Kingery,W.D., Bowen,H.K., and

Uhlmann,D.R. (1991)]. It should be noted that fine grained glass-ceramic can be obtained without use of nucleating agents. However, no paper mentions the mechanism of nucleation and crystallization.

Crystalline phases in these glass-ceramics system are mainly wollastonite ($CaO{\cdot}SiO_2$) [Barbieri,L., Lancellotti,I., Manfredi,T., and Pellacani,G.C.(2001), Barbieri,L., Corradi,A., and Lancellatti,I. (2000)], pyroxene group with chain structure, for example diopside $CaMg(Si_2O_6)$ [Erol,M.,Demirler, U., Kucukbayrak,S., Ersoy,A., and Ovecoglu,M.L.(2003), L., Corradi,A., and Lancellatti,I. (2000), Erol,M., Genc,A., Ovecoglu,M.L.,Yucelen,E., Kucukbayrak,S., and Taptik,Y.(2000), Baebieri,L., Lancellotti,I., Manfredini,T., Queralt,I., Rincon,J.M., and Romeo,M.(1999)] and melilite group with layer structure, for example $(Ca,Na)_2(Al,Mg)(Si,Al)_2O_7$) [Barbieri,L., Ferrari,A.M., Lancellotti,I., and Leonelli,C. (2000)]. The microstructure and orientations of these crystals may provide a relatively high strength of glass-ceramics.

CHAPTER III

CHARACTERIZATION OF FLY ASH

3.1 Chemical composition

The fly ash used here was supplied from " Rayong coal-fired thermal power plant" and appeared to be dark grey in color. The fly ash sometimes contains a small amount of organic material or reducing material which attacks Pt/Rh alloy severly, hence it was calcined to remove these reducing materials. Table 3.1 shows the weight loss of fly ash after calcinations at various temperatures, the weight loss (change) is rather small, but the color changes to light brown from dark grey. This indicates that some organic materials were burned out and oxidized. Finally, fly ash was calcined at 900 ^{o}C for 10 h in fire clay crucible in an electric furnace in air, and cooled to room temperature in the furnace and stored in descicator.

Table 3.1 Weight loss of coal ash after calcinations. -Δ = weight loss

Calcination (^{o}C-10 h.)	Fly Ash			Bottom Ash		
	Before (g)	After (g)	-Δ (%)	Before (g)	After (g)	-Δ (%)
700	10.0128	9.8672	1.4541	10.1005	10.0985	0.0198
800	10.0878	9.7621	3.2287	10.1572	9.4466	6.9960
900	10.0871	9.7409	3.4321	10.1581	9.3834	7.6264

The chemical composition of fly ash was analyzed by XRF method (Chemical Analysis Department, The Siam Research and Development Co., Ltd.). The chemical composition of fly ash is shown in Table 3.2, and those of the other waste materials are also shown.

Table 3.2 Chemical composition (wt%) of fly ash and another waste materials.

Oxide	Chemical composition (wt%)			
	Rayong Thailand	Spanish	Italian	Blast furnace slag
SiO_2	41.62	58.90	55.20	34.00
Al_2O_3	23.11	25.50	7.10	9.90
Fe_2O_3	6.03	6.60	3.80	2.20
CaO	14.92	5.60	23.70	40.60
MgO	1.59	1.10	1.40	3.90
BaO				2.30
MnO				3.60
Na_2O	1.15			0.30
K_2O	1.92			1.90
S				1.90
SO_3	5.42			
TiO_2		1.20	0.30	1.00
LOI	2.80			
Other		0.80	1.30	

It is clear that the composition of fly ash strongly depends on the producing district. This fly ash is composed of SiO_2-Fe_2O_3-CaO-Al_2O_3 with a small amount of R_2O. It should be noted that fly ash contains a considerable amount of SO_3. On the contrary, the blast furnace slag contains a relatively large amount of transition metal oxides.

3.2 Crystalline phase

A powder x-ray diffraction method (XRD) was employed to identify the crystalline phases and to evaluate the percent crystallinity, because the fly ash contains a relatively large amount of glassy phase.

The percent crystallinity was determined according to Ohlberg and Stricklers's method. [Ohlberg,S.M., and Strickler,D.W.(1962)]

The measurement of noncrystalline X-ray scattering has been successfully used to determine the crystallinity of stretched rubber. The crystalline material is formed at the expense of the amorphous phase, the scattering intensity of the amorphous phase will be proportionately reduced on crystallization; if glass is partly devitrified, the loss in amorphous scattering is proportional to the amount of crystalline phase developed. Thus, if I_g is equal to amorphous scattering of the parent glass and I_x is equal to the amorphous scattering of the partly devitrified glass, the following equation can be written:

$$\% \text{ crystallinity of partly devitrified glass} = 100(I_g - I_x) / I_g \qquad (3.1)$$

The actual measurments must be corrected for background scatter, such as that due to the air, the instrument, and the Compton effect. An empirical correction for background was obtained from a mechanical mixture of crystalline compounds chemically equivalent to the parent glass

The concept can be simplified by measurement the noncrystalline scattering intensity at a single value of 2θ. The value of 2θ selected for intensity measurements is obtained by first examining X-ray diffraction patterns of the parent glass, the partly

devitrified glass, and the mechanical mixture of crystalline compounds. A value of 2θ is then chosen at which the noncrystalline scattering intensity is high for the parent glass and at the same time is not overlapped by crystalline peaks in either the partly devitrified sample or the mechanical mixture used for background correction. The working equation then becomes the following:

$$\% \text{ crystallinity of partly devitrified glass} = 100\,(I_g - I_x) / (I_g - I_c) \qquad (3.2)$$

where I_g, I_x and I_c are respectively, the scattering intensities of the parent glass, the partly devitrified sample, and 100% crystalline compounds all measured at the same value of 2θ.

The assumption made in this method which could limit its application. It is assumed that the corrected intensity measured at a single value of 2θ is proportional to the total amorphous X-ray scattering. In addition, the amorphous halo characteristic of the parent glass is assumed to change only with respect to intensity when the glass is partly devitrified.

A further assumption made is that the absorption coefficient of the parent glass does not differ significantly from that for the residual glass. It should be noted that the background correction is at best an approximation.

In general, the validity of the assumption made in this method should be tested as described here for each glass composition under study.

Finally, it should be pointed out that the method is not suitable for measuring crystallinities less than 10 % because a small change in noncrystalline scattering

cannot be measured accurately. For such case, it is advisable to determine first the crystallinity of a sample more than 10% devitrified. A standard sample of known crystalline content is there-by provided. It is then possible to convert to a crystallinity determination based on the measurement of crystalline scattering; this method is more sensitive at low crystallinities.

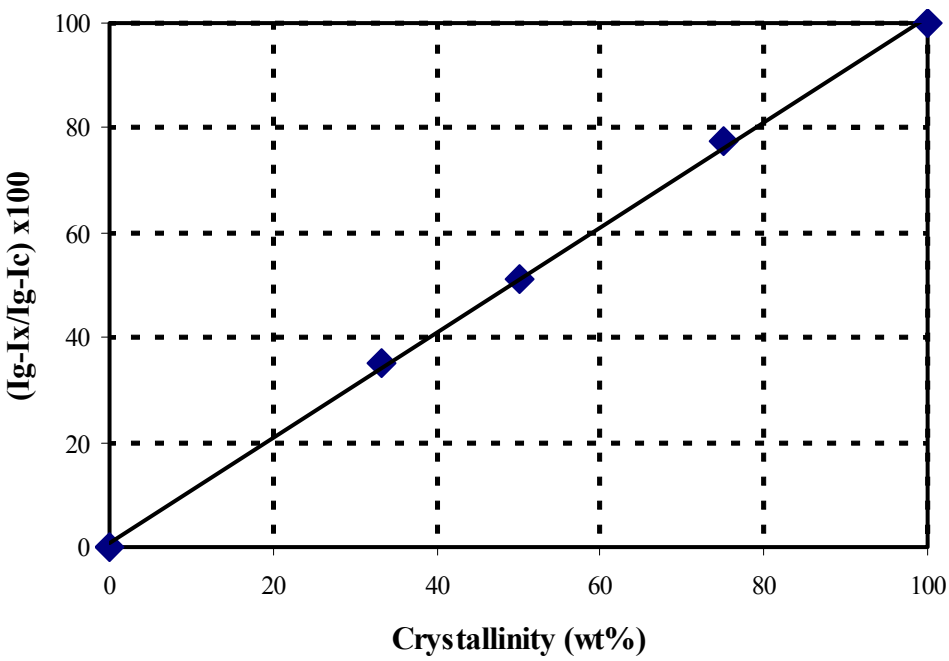

Figure 3.1 Calibration curve for percent crystallinity

Figure 3.1 shows the calibration curve selected from the relative intensity at $2\theta = 23^{o}$. It is found that a good linearity can be obtained.

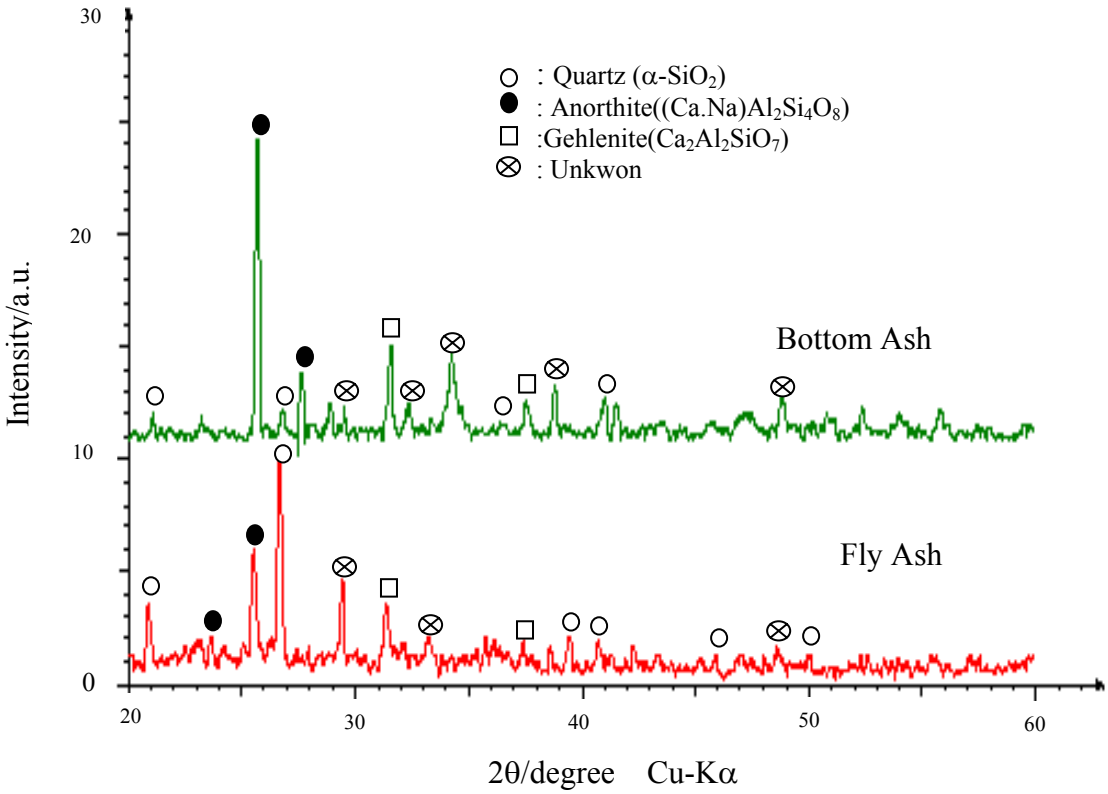

Figure 3.2 XRD patterns of fly ash and bottom ash after calcined at 900 ^{o}C for 10h.

Figure 3.2 shows the XRD pattern of calcined fly ash and bottom ash, and a percent crystallinity and crystalline phase are summarized in Table 3.3.

The fly ash consists of glassy phase with small amount of crystals, α-quartz , anorthite($CaAl_2Si_2O_8$) and gehlenite($Ca_2Al_2SiO_7$). On the contrary, bottom ash was composed of crystals with a small amount of glassy phase.

The main crystal of fly ash is α-quartz with a small amount of glassy phase. Whilst the crystalline phase is a main phase of bottom ash. The percent crystallinity of fly ash and bottom ash are evaluated to be about 26 and 90 % .Percent crystallinity of coal ash is shown in Table 3.3.

Table 3.3 Percent crystallinity of coal ash.

				% Crystallinity	Crystalline phase
	I_x	I_g-I_c	I_g-I_x	$(I_g-I_x)/(I_g-I_c)$x100	
Quartz	0.7			100	Quartz(α-SiO_2)
Glass	3.8	3.1	0	0	-
Fly Ash	3.0	3.1	0.8	25.8	Quartz(α-SiO_2), Anorthite,Gehlenite, Unkwon phase
Bottom Ash	1.0	3.1	2.8	90.3	Quartz(α-SiO_2), Anorthite,Gehlenite, Unkwon phase

I_x : value from XRD pattern

It is considered that the fly ash has been cooled quickly, and bottom ash was cooled slowly to allow the crystallization.

3.3 Appearance by SEM

The appearance of fly ash was observed using scanning electron microscope (SEM, JEOL, JSM 6400). Figure3.3 shows the SEM photos of fly ash.

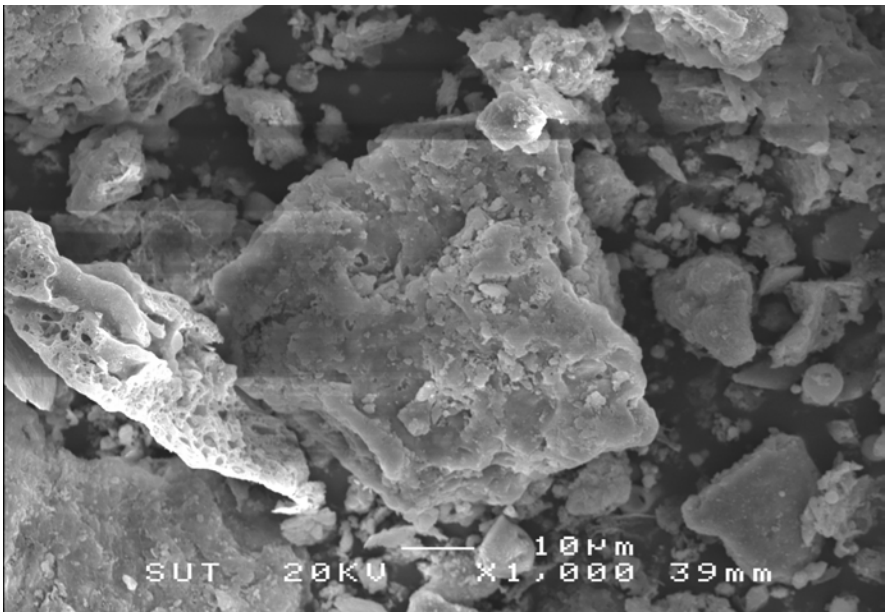

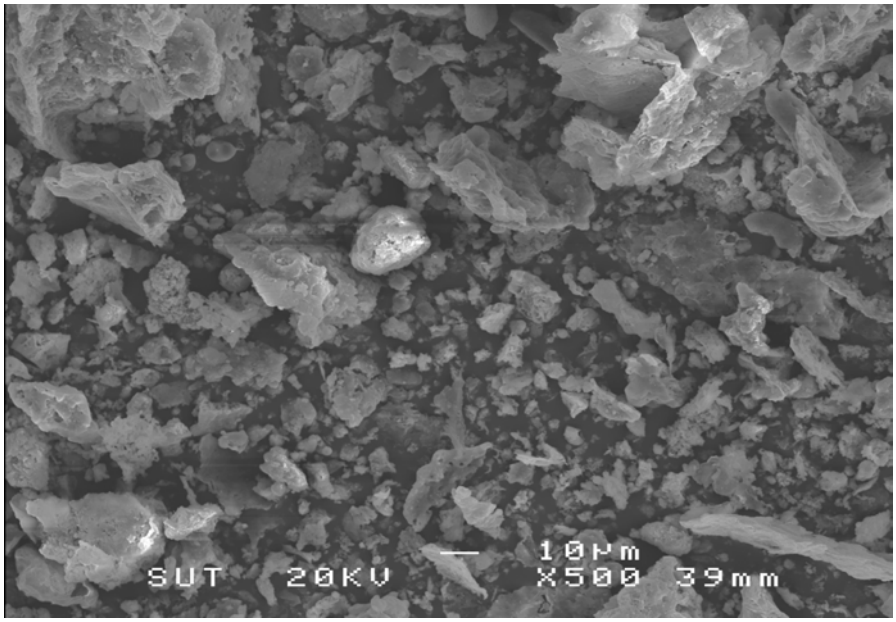

Figure 3.3 SEM photos of fly ash.

The particle size distribution was determined by Laser particle size analyser (Mastersizer Malvern,UK), and is shown in Figure 3-4. Average particle size is about 33μm with a small amount of fine particles (smaller than 1 μm.)

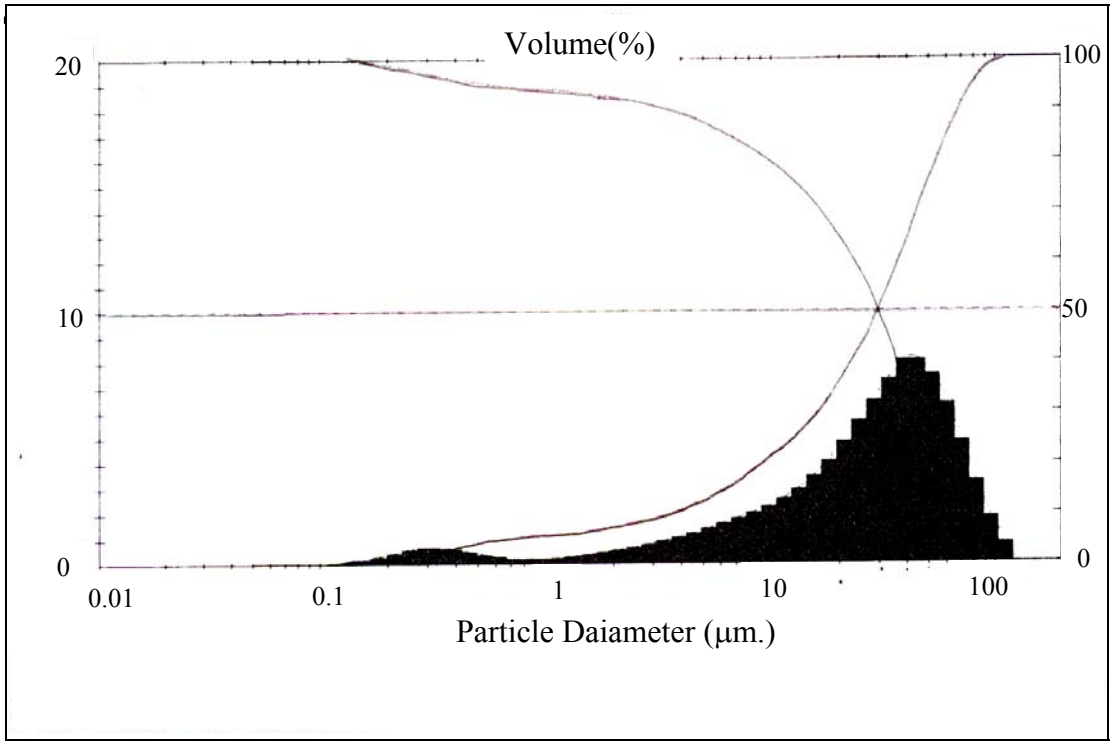

Figure 3.4 Particle size distribution of calcined fly ash.

CHAPTER IV

DETERMINATION OF TARGET GLASS COMPOSITION

This fly ash is composed of SiO_2-Al_2O_3-CaO system with a considerable amount of Fe_2O_3 and SO_3 as shown in Table 4.1. Considering the composition, fly ash might be form as a glass by itself, and the dark brown to black color was be expected. This kind of glass or glass-ceramics may be useful and suitable for the application of floor tile or side wall cladding. However it is not applicable for tableware etc., because of its deep color. On the other hand, fly ash should be introduced into glass as raw materials as large amount as possible.

4.1 Base glass composition

Thus the base composition which provides easy melting and crystallization would be selected based on SiO_2-Al_2O_3-CaO system. The next glass composition (Table 4.1) was chosen according to above discussion. The Na_2O component was introduced for easy melting as a flux.

Table 4.1 Chemical composition (wt%) of base glass.

SiO_2	Al_2O_3	Fe_2O_3	MgO	CaO	Na_2O	K_2O
60.1	8.1	2.2	4.6	18.0	5.1	0.7

About 35 % of fly ash can be introduced as a raw material to 100 g of glass. CaF_2 (nucleating agent) and spodumene (reduced thermal expansion coefficient) were added by additional weight%.

The crystallization behavior of this glass is not clear yet, sometimes the suitable nucleating agents would be required for crystallization. These nucleating agents also should provide no coloration.

4.2 Effect of CaF_2 (Series I)

As mentioned previously, usually the nucleating agent has not been used in the glass-ceramics produced from fly ash. However the crystallization behavior of this glass is not clear yet, the effect of CaF_2 was investigated as a nucleating agent, and 1~3 mass % CaF_2 was added by additional weight. These glasses are expressed as Serie I.

4.3 Effect of spodumene (Series II)

In order to reduce the thermal expansion coefficient, spodumene was introduced into the glass Series II. The batch composition is given in Table 4.2

Table 4.2 Batch composition of glasses.

Raw Material	Series I				SeriesII		
	G-0	G-1	G-2	G-3	G-3	G-4	G-5
Fly Ash	35.0	35.0	35.0	35.0	35.0	35.0	35.0
Sand	45.5	45.5	45.5	45.5	45.5	45.5	45.5
Dolomite	15.0	15.0	15.0	15.0	15.0	15.0	15.0
Limestone	14.0	14.0	14.0	14.0	14.0	14.0	14.0
Soda Ash	8.0	8.0	8.0	8.0	8.0	8.0	8.0
CaF_2*	0	1.0	2.0	3.0	3.0	3.0	3.0
Spodumene*	0	0	0	0	0	10	20

* ; additional weight %

CHAPTER V

EXPERIMANTAL PROCEDURE

5.1 Sample Preparation

The glass compositions used are shown in Table 4.1. A calcined fly ash, factory grade spodumene, silica sand, dolomite, limestone and reagent grade chemicals of Na_2CO_3 and CaF_2(Carlo Erba) were used as raw materials.

Batches corresponding to 100 g of glass were dry mixed thoroughly in a ball mill for 30 minutes. Then they were melted in 100 cc Pt/Rh10 crucible at 1450 ^oC for 1 hour in an electric furnace in air, and then poured onto iron plate. They were then annealed at 750 ^oC for 5 hours and cooled to room temperature in the furnace.

Rods about 5 mm diameter were freshly drawn and cut into about 5 cm long samples for strength measurement. The samples were then annealed at 750 ^oC for 5 hours and cooled to room temperature in the furnace.

The glasses were heat treated for crystallization at various conditions after the first heat treatment at 750 ^oC for 10 hours.

5.2 DTA

DTA run was carried out routinely with Perkin-Elmer DTA-7 at the heating rate of 10 K/min.. The powdered specimens passed #100 were used. DTA curve will

show Tg (glass transition temperature), Tonset (initial crystallization temperature) and Tc (crystallization temperature)

5.3 Thermal expansion and Density

Thermal expansion coefficient (α), glass transition point (Tg) and yielding point (Yp) of glass and glass-ceramics were measured with fused silica single push rod type dilatometer (Netzsch DIL 402 EP) at heating rate of 5 K/min.

The density of glass and glass-ceramics were measured by He gas substitution method with Accupyc 1330 (Micromeritics) at room temperature.

5.4 X-ray powder diffraction (XRD)

XRD was carried out for identification of crystalline phase and determination of percent crystallinity under the condition of 40 KV- 30mA, Cu-Kα, 0.02 ^{o}/step, 0.5 sec/ step , 2θ = 20-60 ^{o} (Bruker, AXS Model D5005). The details of the determination of percent crystallinity were already mentioned in chapter 3.2.

5.5 Scanning electron microscope observation (SEM)

The structure of glass and glass-ceramics was observed by scanning electron microscope(SEM JEOL JSM 6400).The fractured surface was etched by 1% HF solution for about 2 minutes in ultrasonic bath at room temperature.

5.6 Strength measurement

The fracture strength of 20 rod specimens of annealed glasses and 20 rod specimens of glass-ceramics were measured by using Instron Model 5569 according to ASTM C-158. The three-point bending method was employed and the surface of the 10 specimens was abraded by 230 mesh SiC abrasive paper before the measurement, and the strength of 10 non-abraded specimens was also measured. The span length and loading rate were 30 mm and 10 mm/ min respectively.

For hardness of glass-ceramics could be observed by fracture strength of abraded and non-abraded specimens almost showed the same value that meaning of surface hardness of specimens might be high, resulting in scratch free surface.

The fracture strength is calculated by below equation

$$\text{Fracture strength} = 8PL/\pi\phi \qquad (5.1)$$

P = breaking load (N)

L = span length (mm.)

ϕ = average diameter of specimen (mm.)

5.7 Chemical Durability

Glasses and glass-ceramics were ground, sieved between 18-30 mesh, washed by acetone and subsequently ethanol. Afterwords, they were then dried at 120 ^{o}C and stored in desicator.

The density gram specimens were immersed in 100 cc. of 1N of HCl at 90°C for 5 hours and the other set of specimens were immersed in 100 cc.of 1N of NaOH at

$90^{o}C$ for 5 hours, and then their weights were measured before and after the treatment.

The weight loss is calculated by below equation

$$\% \text{ weight loss} = (W_1 - W_2)/ W_1 \times 100 \quad (5.2)$$

W_1 = weight before leaching

W_2 = weight after leaching

5.8 Thermal shock resistance

Thermal shock resistance is examined according to ASTM no. C 554-93. The oven temperature was operated from 100 to 200 ^{o}C, increase 10 ^{o}C step by step and water container was hold water at 20 ^{o}C before quenching (10 cm^3 of water/g of ware). The three rod specimens were used in each composition. Consider only failures that are visible to the naked eye.

And the calculation of ΔT, this below equation was used

$$\sigma = E \cdot \alpha \cdot \Delta T / (1-\mu) \quad (5.3)$$

Where E = Young's modulus for glass and glass-ceramics = 70 Gpa.

α = thermal expansion coefficient

ΔT = temperature difference

μ = Poisson's ratio for glass and glass-ceramics = 0.3

and σ = the stress arisen by extreme temperature change

for E and μ from Arun,K.V. (1994).Fundamentals of inorganic glassed.

CHAPTER VI

RESULTS

6.1 Properties of glasses

Bubble free and dark green glasses were prepared. The various properties of glasses are summarized in Table 6.1.

6.1.1 Thermal properties

Glass transition temperature (Tg) in Series I glasses decreases slightly with increase in CaF_2 content. Tg of Series II glasses decreases with increase in the amount of spodumene. The dilatometric softening point (Yp), and thermal expansion coefficient (α) do not change so much with composition. α of series II glasses is smaller than that of series I glasses.

6.1.2 Density

Figure 6.1 shows the density of both series of glasses. The density of Series I glasses increases gradually with increase in CaF_2 content. On the contrary, the density of Series II glasses decreases markedly with increase in the amount of spodumene.

Table 6.1 Properties of glasses studied.

Glass No.	Additives[1]		Appearance	Thermal Properties			Density (g/cm^3)	Chemical durability[3]		Fracture strength σ^4 (MPa)
	CaF_2 (wt%)	Spodumene (wt%)		Tg (^oC)	Yp (^oC)	α^2 ($x10^{-7}/K$)		Acid (-Δ %)	Alkali (-Δ %)	
G-0	0	0	Dark green	655	702	95	2.659	1.4480	-0.9626	100.4±38.8 70.5± 39.1
G-1	1	0	Dark green	653	693	95	2.655	1.2025	-0.5197	111.6±39.8 78.3±33.9
G-2	2	0	Dark green	642	704	95	2.665	0.9379	0.5549	155.9±55.4 131.4±52.8
G-3	3	0	Dark green	630	691	85	2.692	1.2104	0.1263	124.5±48.5 98.5±40.3
G-4	3	10	Dark green	635	695	85	2.626	1.0538	-0.7118	120.5±46.5 100.1±36.8
G-5	3	20	Dark green	615	690	85	2.605	0.9115	-0.8713	115.6±40.4 110.7±44.3

1 Additional weight %

2 α : 100-300 ^oC

3 % change in weight(positive value = weight loss, negative value = weight gain)

4 upper : non-abraded, lower : abraded (320# abrasive paper)

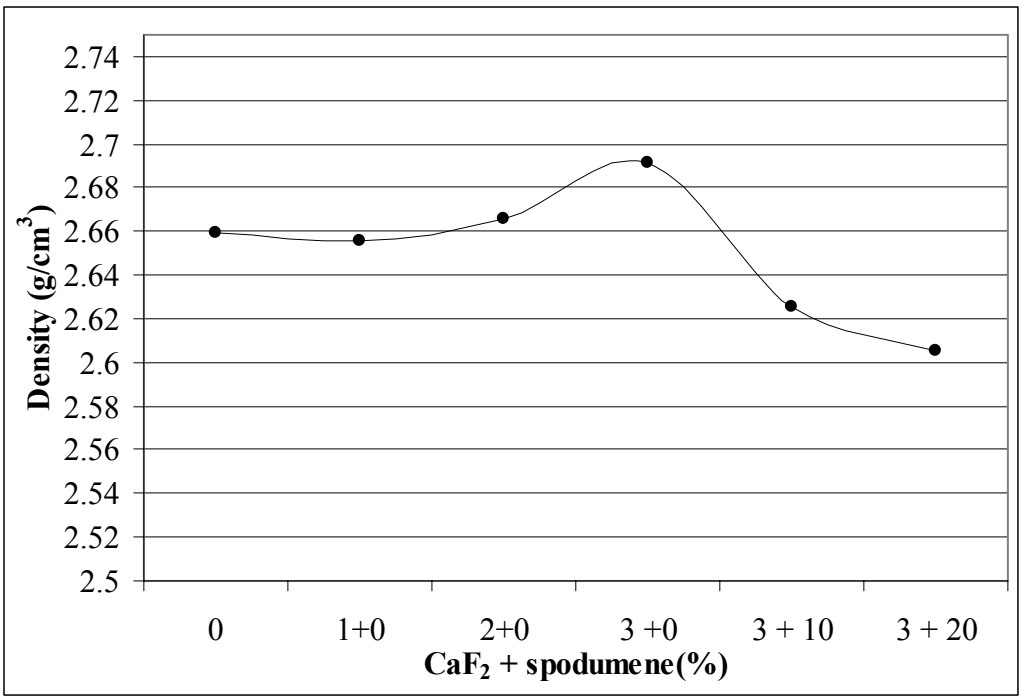

Figure 6.1 Density of series I and II glasses.

6.1.3 Chemical durability

The acid durability of Series I and II glasses increase gradually with increase in the amount of CaF_2 and spodumene contents as shown in Figure 6.2.

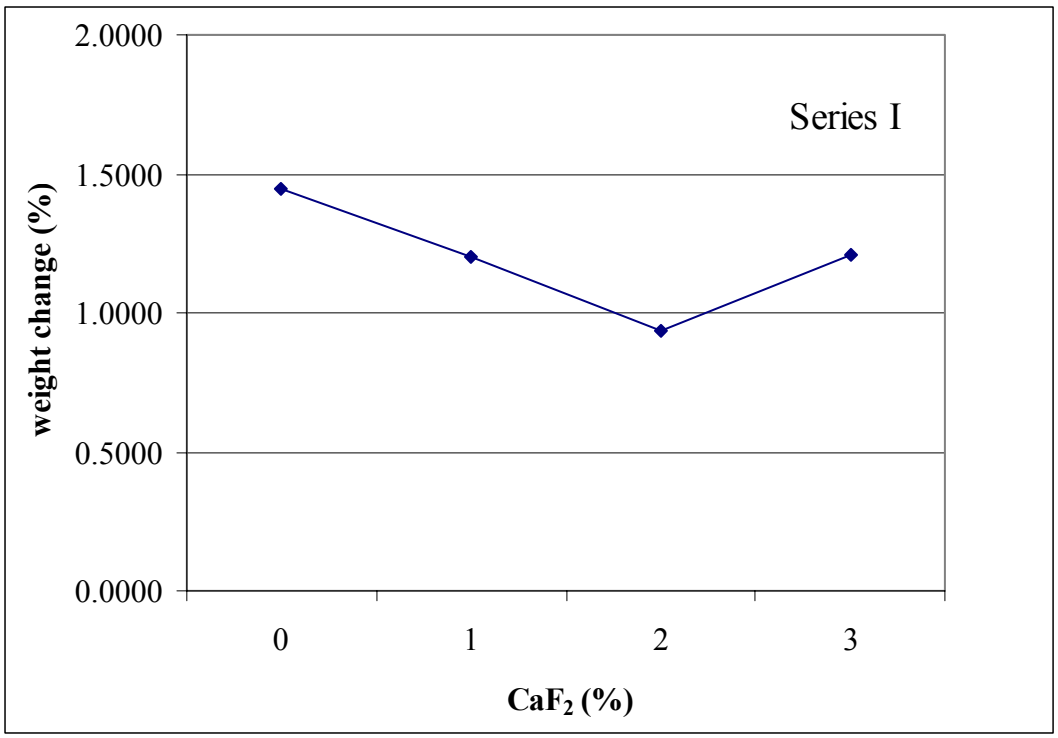

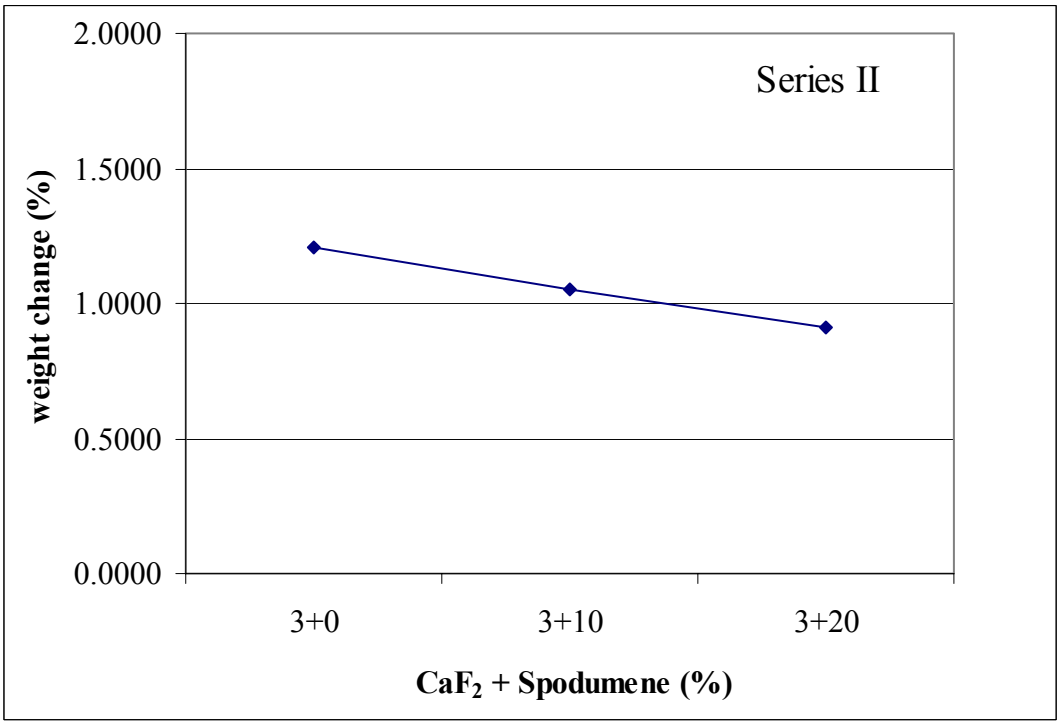

Figure 6.2 Acid durability of series I and II glasses.

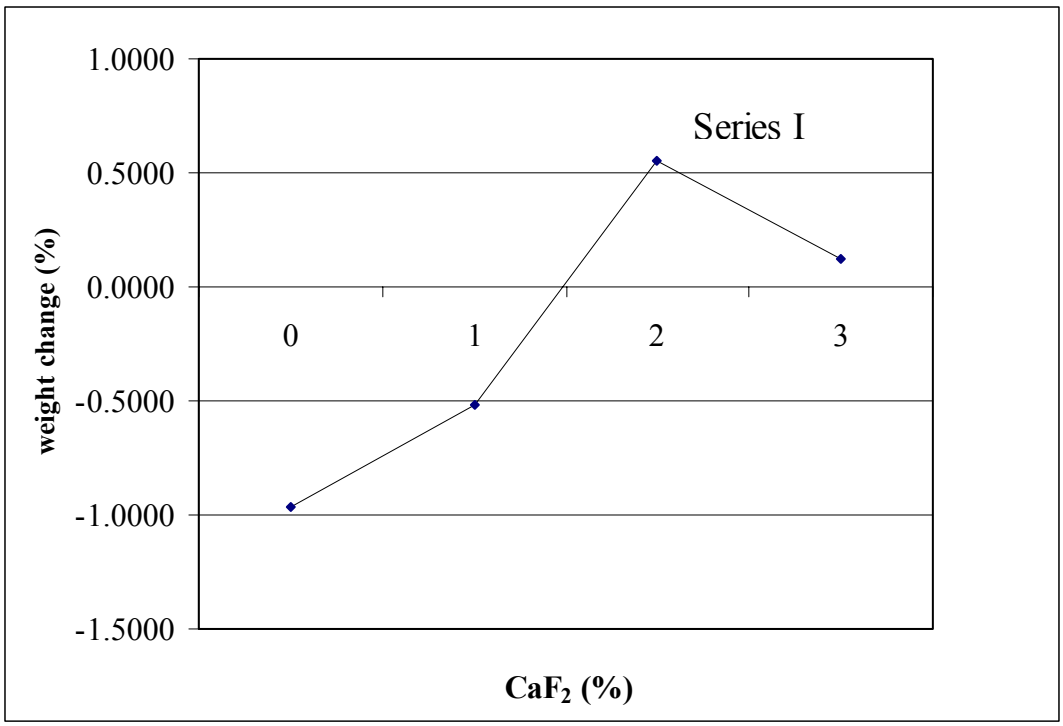

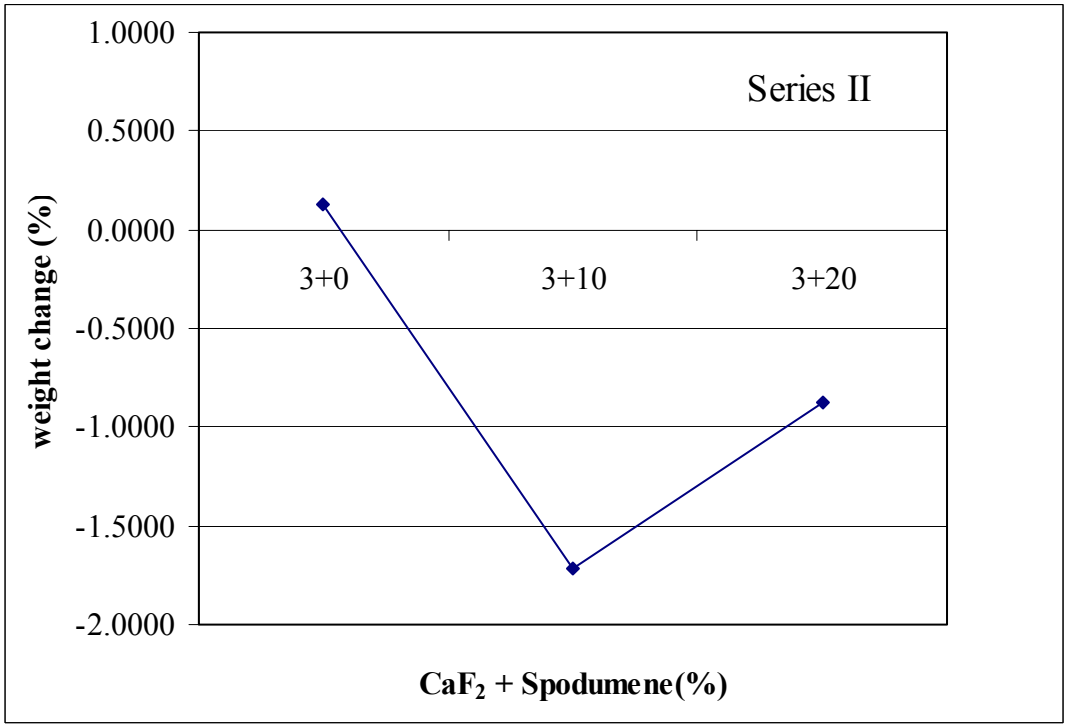

Figure 6.3 Alkaline durability of series I and II glasses.

The alkaline durability of Series I glasses decreases with increase in the amount of CaF_2. On the other hand in Series II glasses, the alkaline durability shows the complicated features, it increases at first and then decreases. It should be noted that the weight gain is observed in the same cases.

6.1.4 Fracture Strength

Figure 6.4 shows the fracture strength of series I glasses. The measured fracture strength scatters very much and the systematic change cannot be observed with composition. The average values are estimated to be about 130 MPa for non-abraded specimens and about 100 MPa for abraded specimens. The fracture strength of abraded specimens were about 30% lower than that of non-abraded specimens.

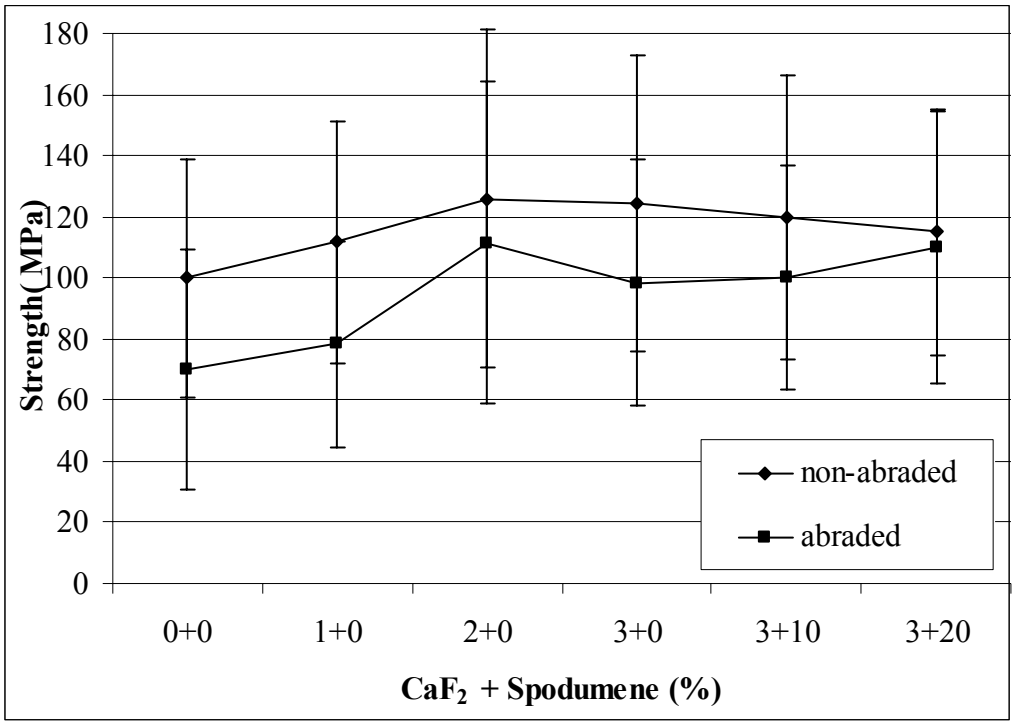

Figure 6.4 Fracture strength of series I and II glasses.

6.2 Phase Separation and Crystallization

Figure 6.5 shows DTA curves of series I and II glasses and DTA results are summarized in Table 6.2. The exothermic peak is observed at around 900°C, due to crystallization.

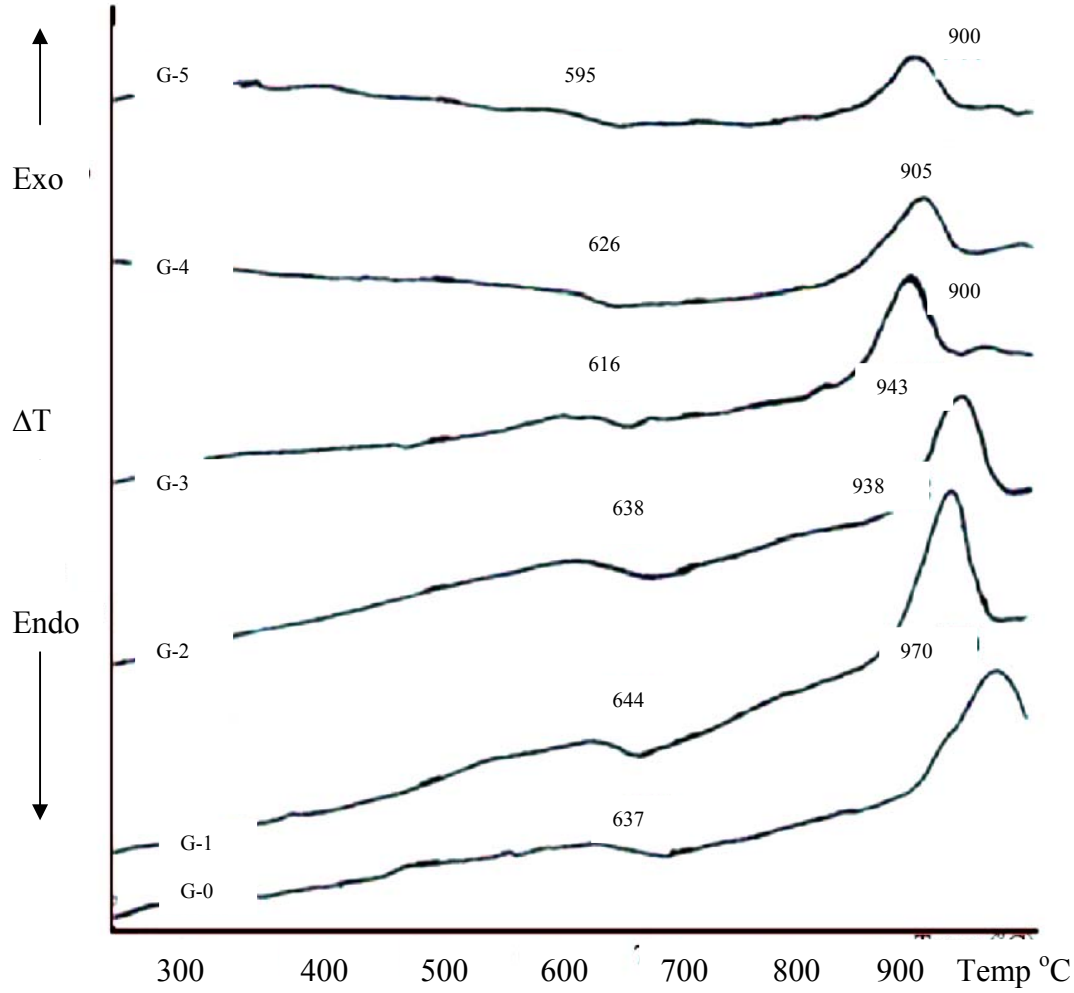

Figure 6.5 DTA runs of glasses. Heating rate : 10K/min

Table 6.2 Thermal properties of glasses and glass-ceramics studied.

No.	Additives[1]		Glass						Glass-ceramics[2]
			Dilatometer			DTA			Dilatometer
No.	CaF_2 (wt%)	Spodumene (wt%)	Tg (^oC)	Yp (^oC)	α^2 ($x10^{-7}/K$)	Tg (^oC)	To (^oC)	Tc (^oC)	α^2 ($x10^{-7}/K$)
G-0	0	0	655	702	95	637	910	970	90
G-1	1	0	653	693	95	644	886	938	105
G-2	2	0	642	704	95	638	894	943	100
G-3	3	0	630	691	85	616	860	900	85
G-4	3	10	635	695	85	626	860	905	85
G-5	3	20	615	690	85	595	860	900	85

1 Additional weight %

2 α : 100-300 ^oC

3 Heating condition 750^oC-10h, 950^oC-5h.

6.2.1 Phase separation

SEM photos of Series I and II glasses are shown in Figure 6.6(a) and Figure 6.6(b), respectively.

A very fine particle (white spots in photos), smaller than 100 nm, and a certain structural fluctuation can be observed in series I glasses. Since XRD confirms no diffraction peaks (Figure 6.7a), this structural fluctuation seems to be phase separation, and their structure are isolated droplet type. However, no systematic structural change with composition is observed. This indicates that CaF_2 does not affect on the phase separation.

On the contrary, in Series II glasses, three dimensional interconnected type phase separation can be observed clearly. The size of the phase separated structure may be about 100 nm. The structure does not change with spodumene content, but the spodumene affects the phase separation dramatically.

6.2.2 Crystallization

It is seen that the exothermic peaks appeared in DTA curves (Figure 6.5), and hence all glasses might be crystallized by further heat treatment.

Both the onset (To) and peak(Tc) temperature decrease with increase in the amount of CaF_2 content in series I glasses. This indicates that CaF_2 affects on the crystallization process in this glass system. On the other hand, the considerable change in onset and peak temperature cannot be observed in series II glasses.

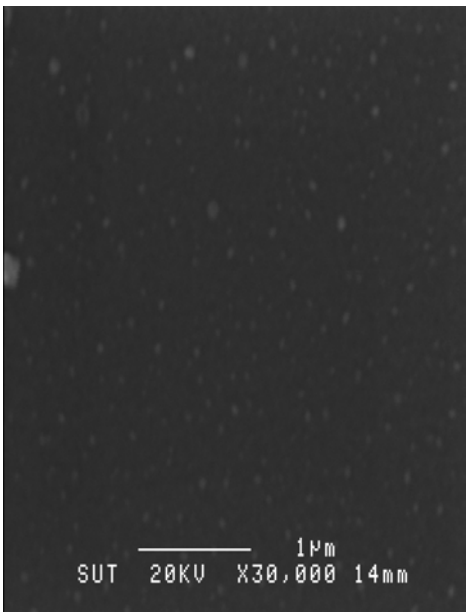

1) CaF_2 = 0 %

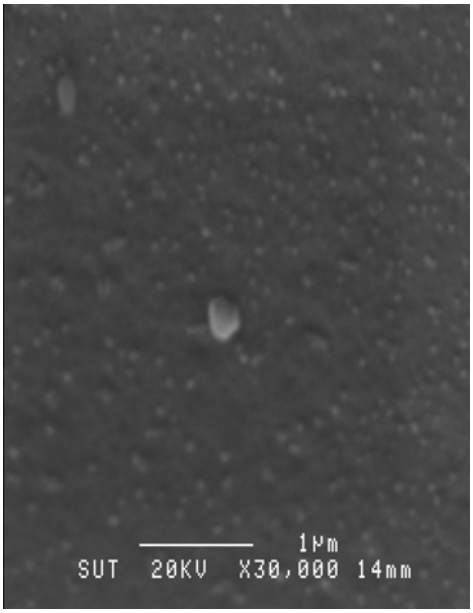

2) CaF_2 = 1 %

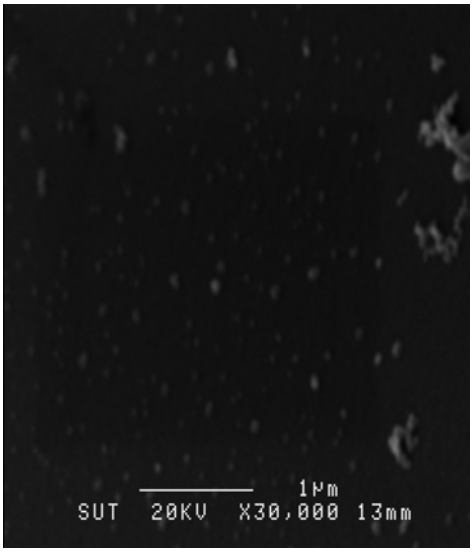

3) CaF_2 = 2 %

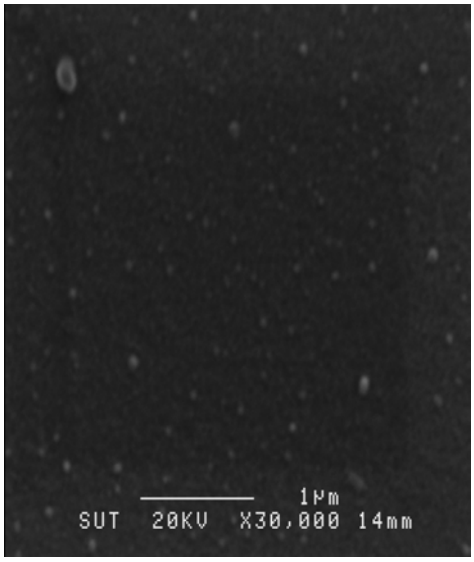

4) CaF_2 = 3 %

Figure 6.6 (a) SEM photos of series I glasses.1st heat treatment 750°C for 10 h.

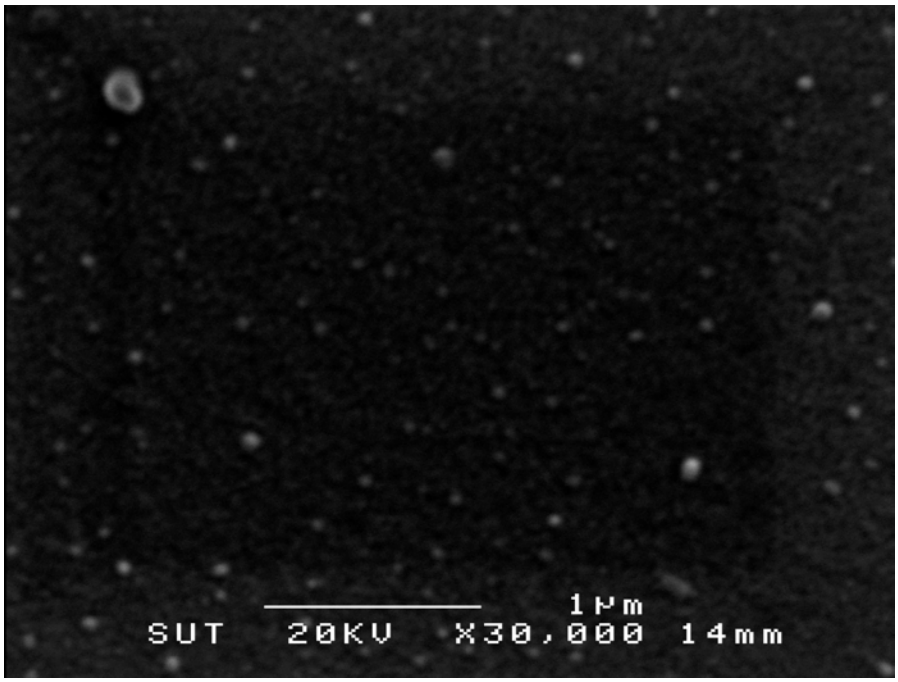

1) CaF_2 = 3

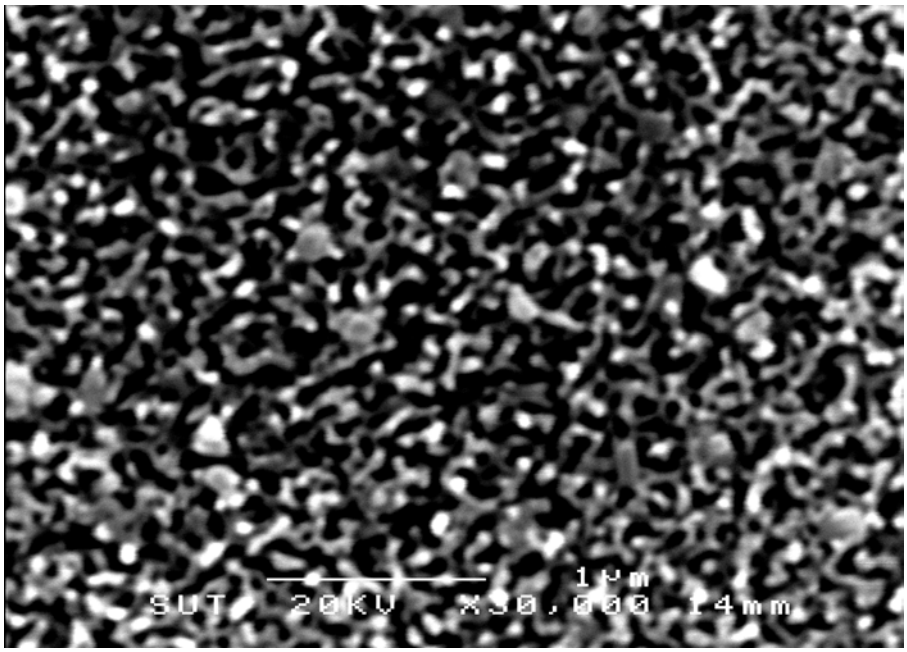

2) CaF_2 = 3 % + Spodumene 10 %.

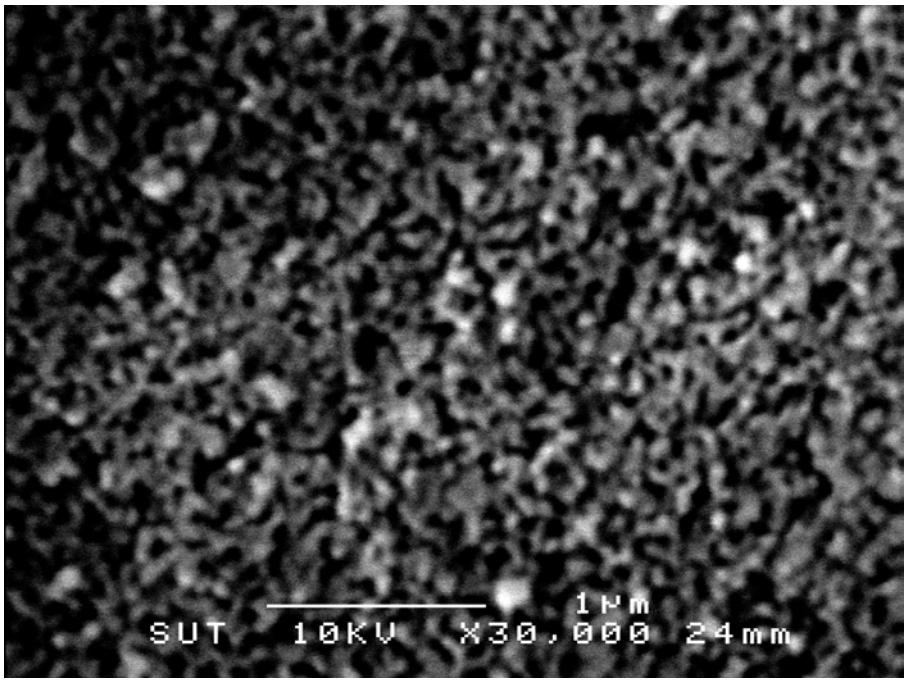

3) CaF_2 = 3 % + Spodumene 20 %

Figure 6.6 (b) SEM photos of series II glasses. 1st heat treatment 750°C for 10 h.

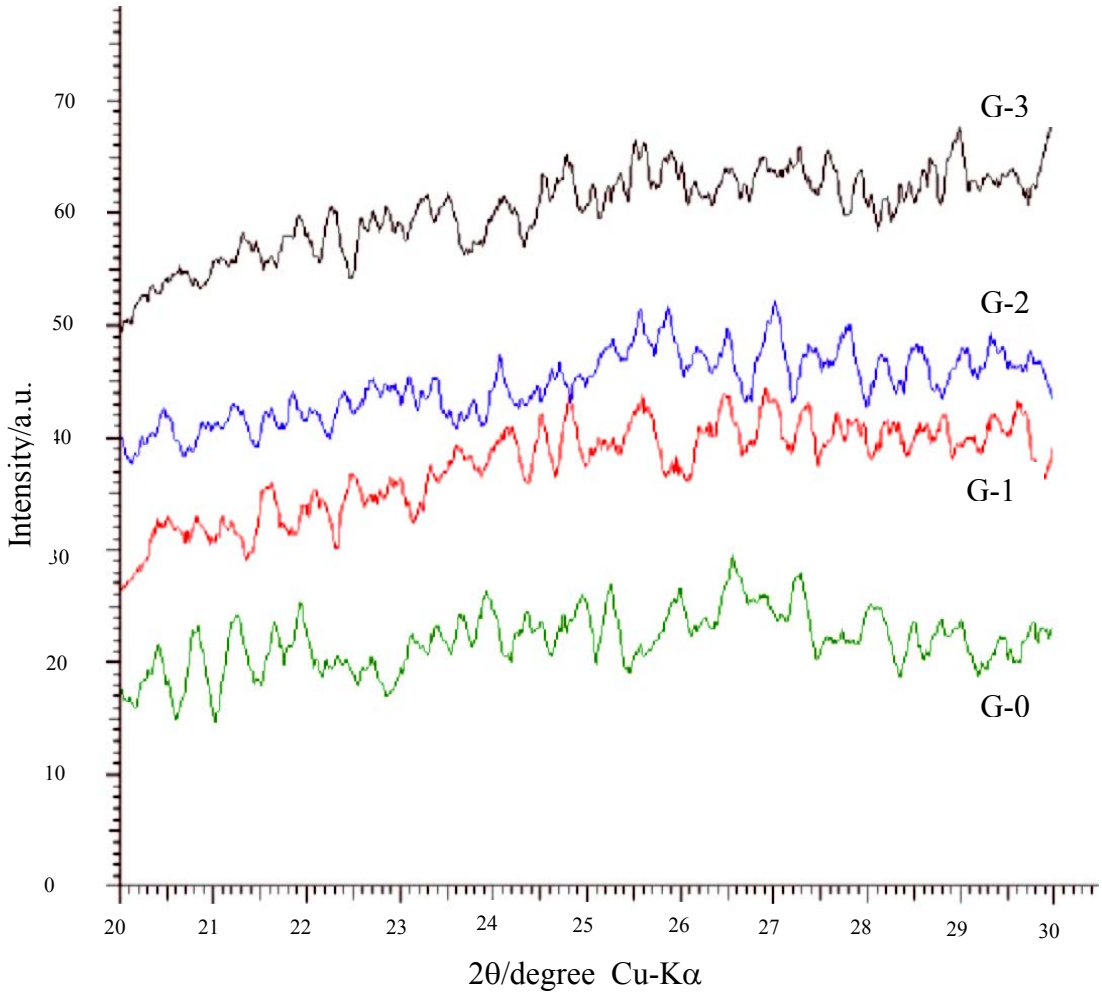

Figure 6.7(a) XRD pattern of series I glasses after heat treatment 750°C for 10 h.

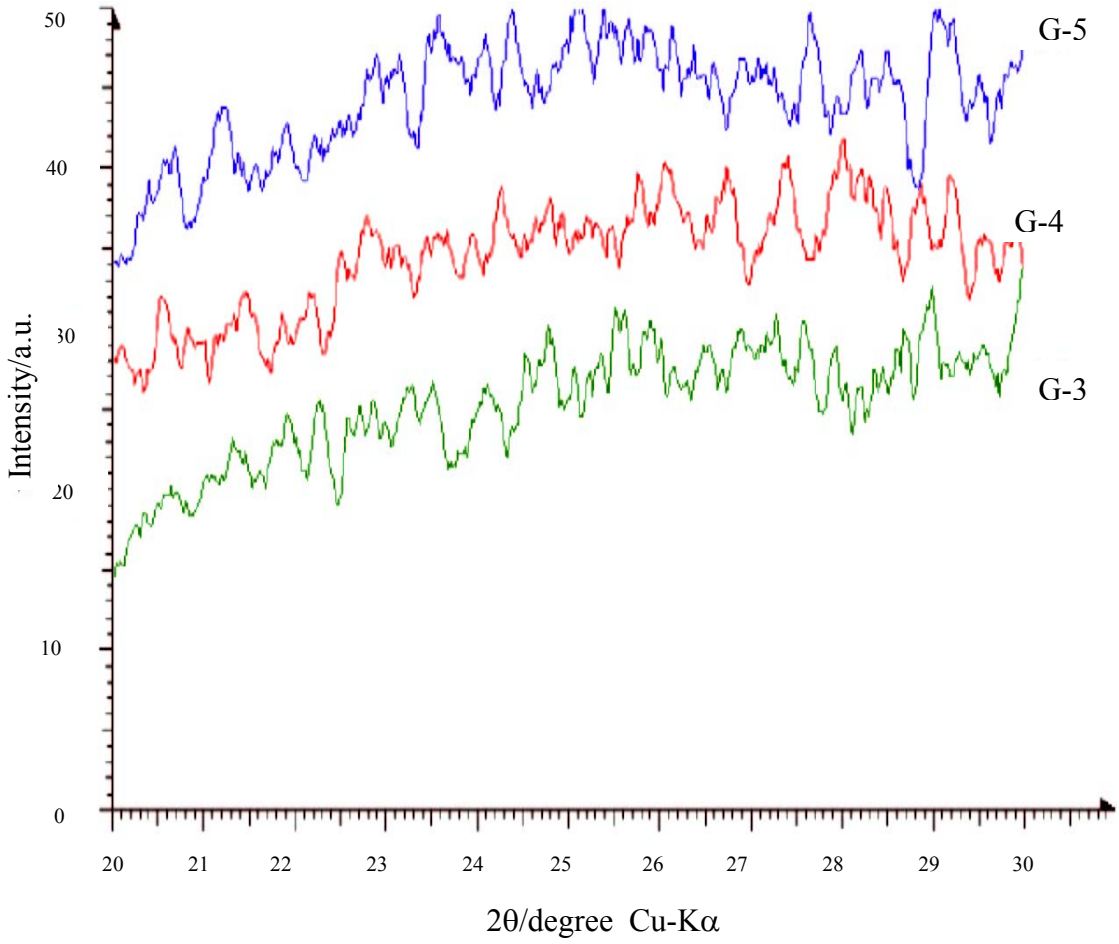

Figure 6.7(b) XRD pattern of series II glasses after heat treatment 750°C for 10 h.

G-0 glass shows only surface crystallization, whilst other glasses exhibit bulk crystallization.

Figure 6.8 shows XRD patterns of G-1 to G-5 glass-ceramics heated at 750°C-10h for nucleation and 950°C-5h for crystallization. Three kinds of crystals, wollastonite($CaSiO_3$), augite($Ca(Mg,Fe)Si_2O_6$) and anorthite($CaAl_2Si_2O_8$), are detected in G-0 to G-3 glass-ceramics. However, in G-4 and G-5 glass-ceramics, wollastonite($CaSiO_3$) and spodumene($LiAl(SiO_3)_2$) crystals are observed.

Figures 6.9 a and b show SEM photos of these glass-ceramics. The rod-like crystal precipitated and it might be wollastonite($CaSiO_3$). In G-3 to G-5 glass-ceramics this rod-like crystal grew well in random direction. The crystallization behavior of G-3 and G-5 glasses was investigated in detail.

Figure 6.10 and Table 6.3 show the relationship between percent crystallinity and 2nd heat treatment temperature at various conditions in G-3 and G-5 glasses after 1st heat treatment at 750°C for 10h. It was the example for studying crystallization behavior.

The percent crystallinity of G-3 glass increase with increase in temperature, reached the maximum at about 1000°C and then decreases again. The percent crystallinity of G-5 glass, however, decreases monotonically with increase in temperature. This indicates that the maximum crystallization temperature of G-5 glass may be below 900°C.

Figures 6.11a and b show XRD patterns of G-3 and G-5 glass-ceramics heat treated at various temperatures. In G-3 glass-ceramics, wollastonite-like crystal precipitates first, and anorthite and augite crystal starts to precipitate at higher temperature. Finally, wollastonite, augite and anorthite crystals coexist at high temperature.

A similar behavior can be observed in G-5 glass-ceramics, and finally wollastonite, anorthite and spodumene crystals are observed.

Figure 6.12 shows SEM photos of G-3 glass-ceramics heat treated under various conditions. It is clearly seen that rod-like crystal precipitates at random direction and grew with increasing temperature. The aspect ratio of this crystal is approx 5 to 10.

Table 6.3 Crystallization behavior of GC-3 and GC-5 studied.

No.	Heating Condition (^{o}C-hr.)	Crystalline Phase[1]	Percent Crystallinity	Crystallization Behavior
G-3	750-10,930-5	W	-	Surface
	750-10,950-5	W	27.9	Bulk
	750-10,1000-5	W, An, Au	51.2	Bulk
	750-10,1050-5	W, An, Au	44.2	Bulk
	750-10,1100-5	W, An, Au	37.2	Bulk
G-5	750-10,930-5	W, An, Sp	59.0	Bulk
	750-10,950-5	W, An, Sp	53.9	Bulk
	750-10,1000-5	W, An, Sp	48.7	Bulk
	750-10,1050-5	W, An	35.9	Bulk
	750-10,1100-5	W, An	30.8	Bulk

W, An, Au, Sp = Wollastonite, Anorthite, Augite, Spodumene

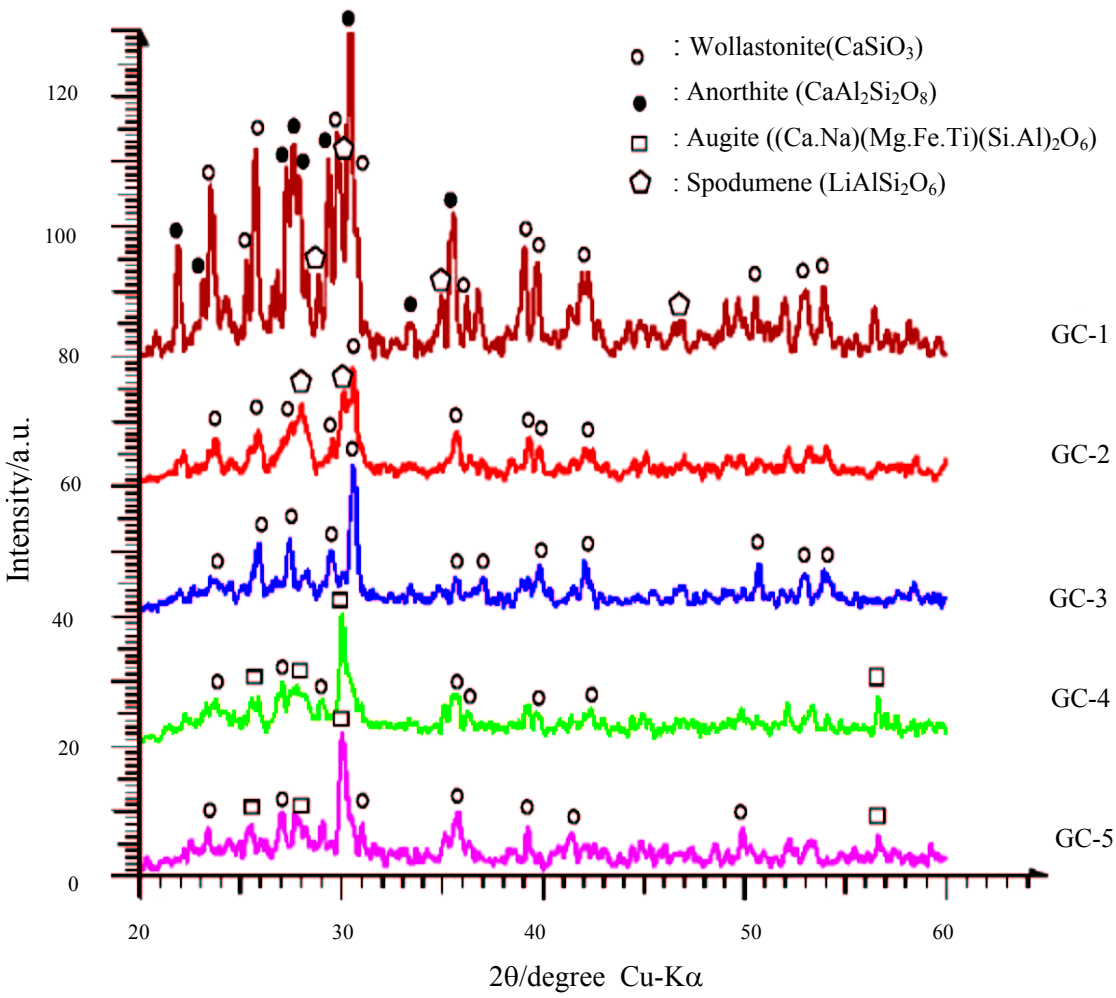

Figure 6.8 XRD patterns GC-1 to GC-5 glass-ceramics. 750°C-10 h , 950°C-5 h.

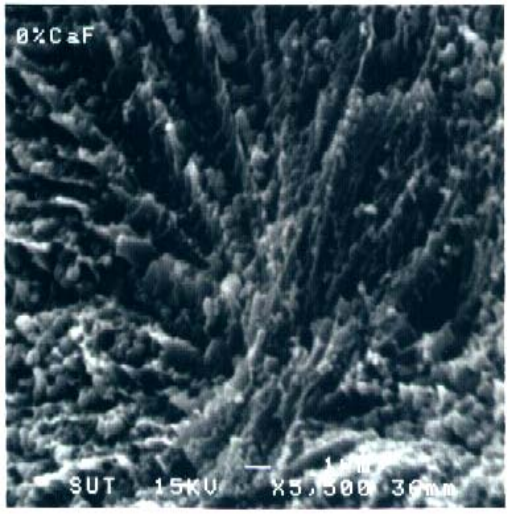

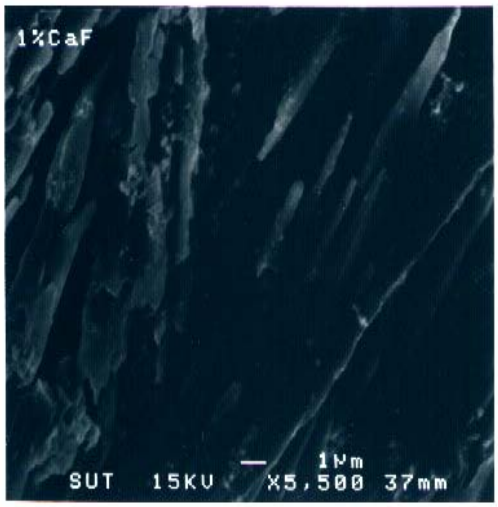

1) GC-0

2) GC-1

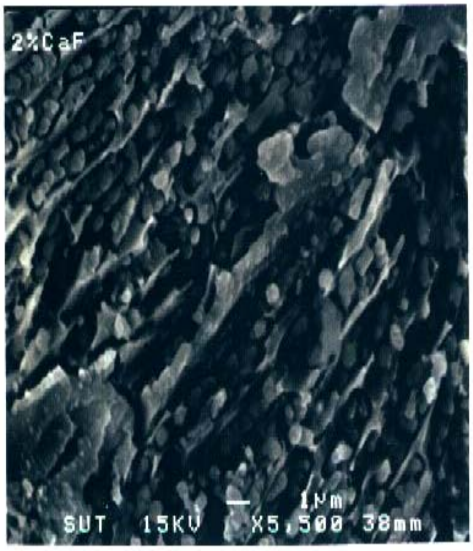

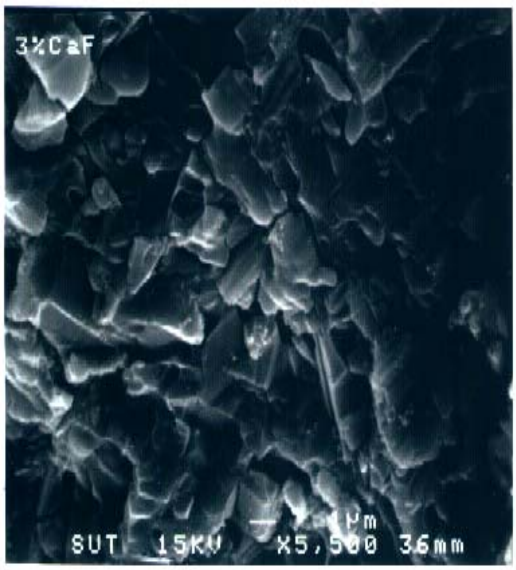

3) GC-2

4) GC-3

Figure 6.9(a) SEM photos of series I glass-ceramics.

heating condition; 750°C-10h, 950°C-5h.

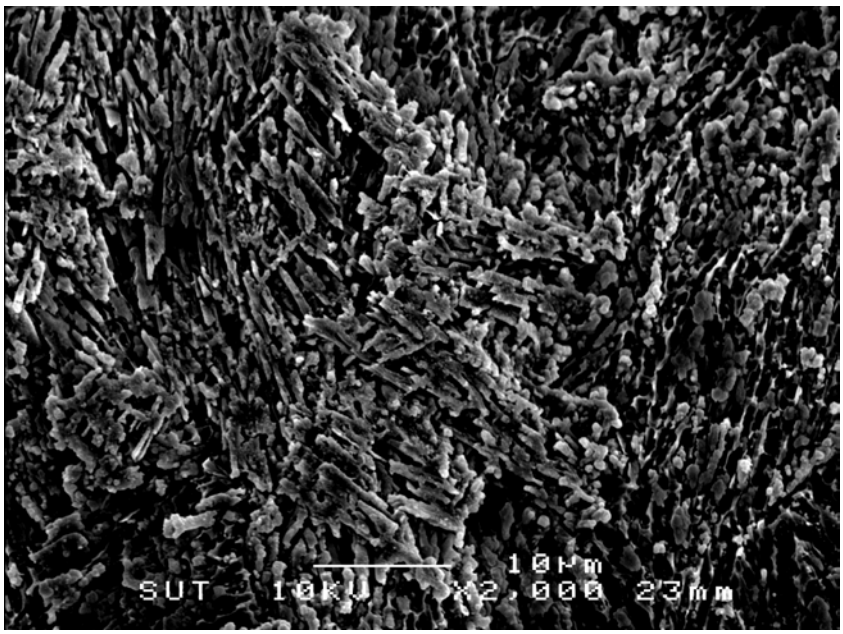

a) GC-3

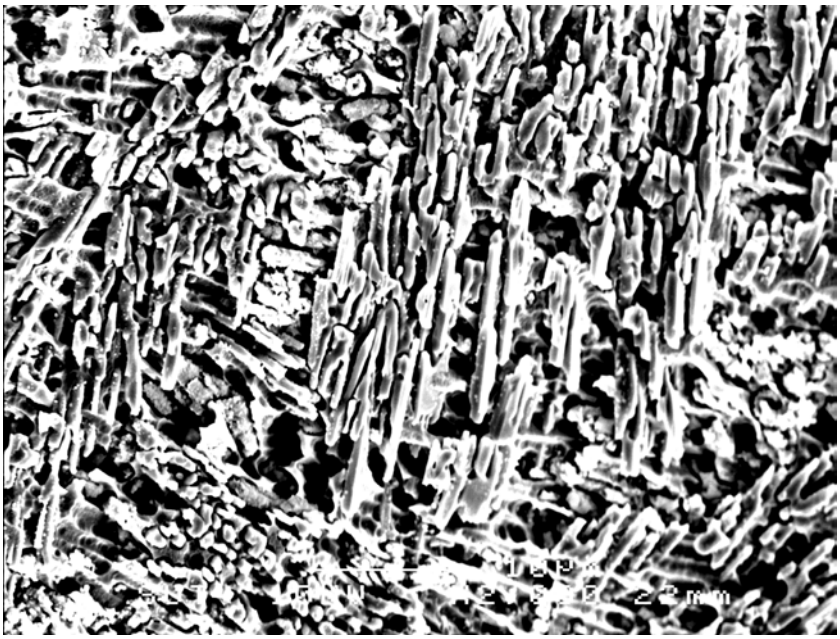

b) GC-4

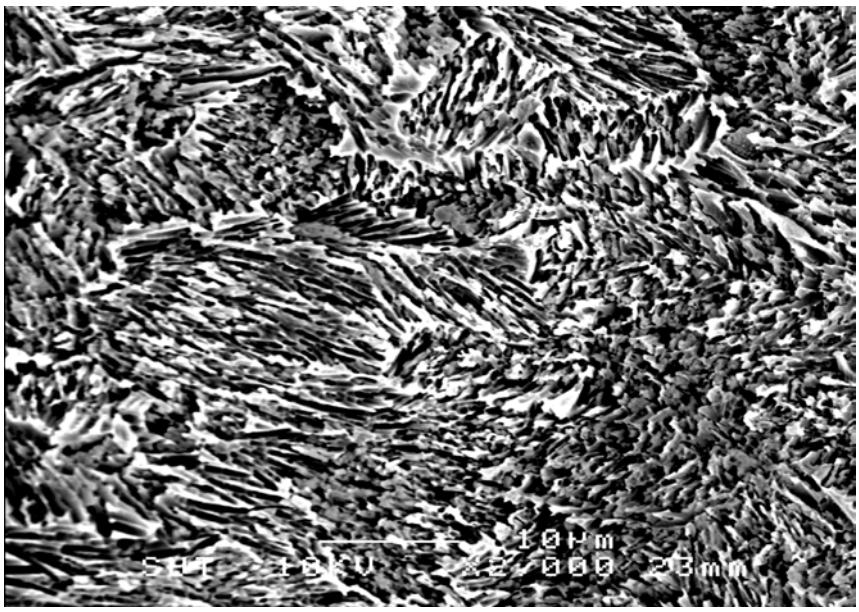

c) GC-5

Figure 6.9(b) SEM photos of serie II glass-ceramics.

heating condition; 750°C-10h, 950°C-5h

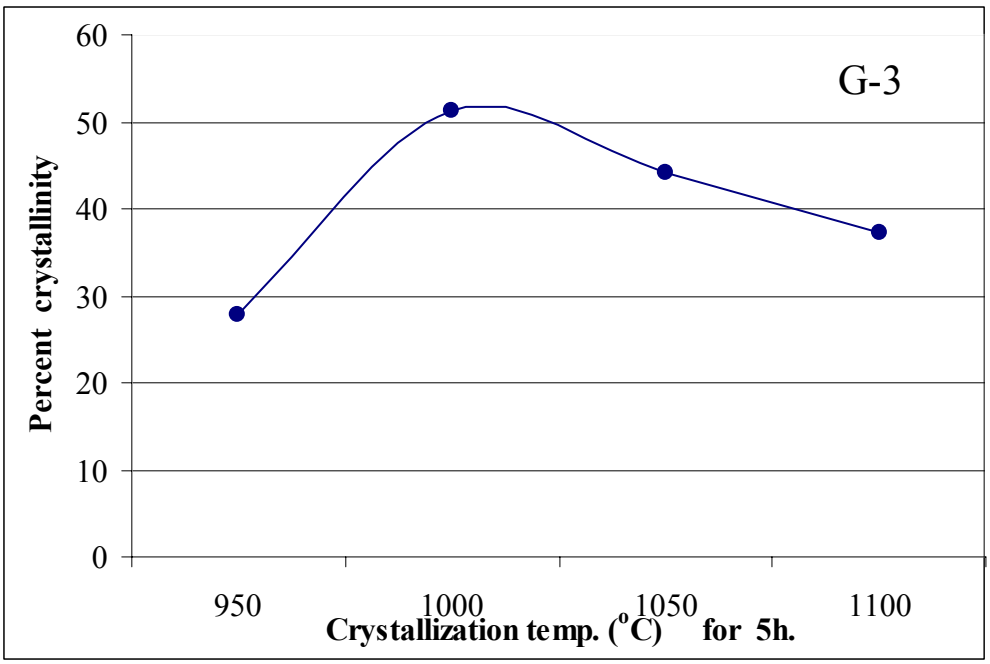

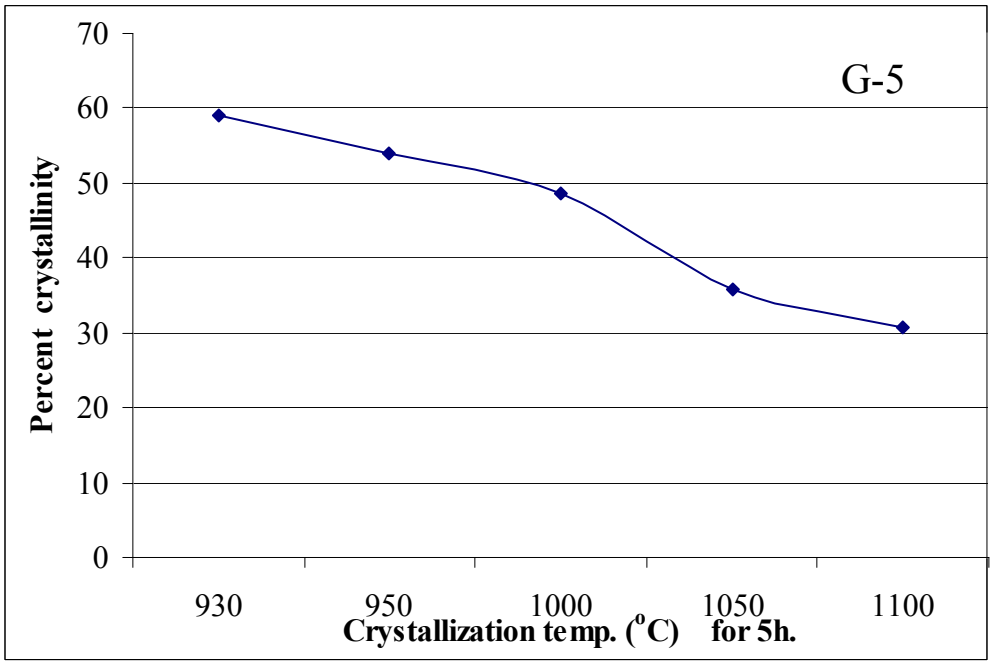

Figure 6.10 Relationship between percent crystallinity and heating temperature at various condition after 1st heat treatment at 750°C-10h.

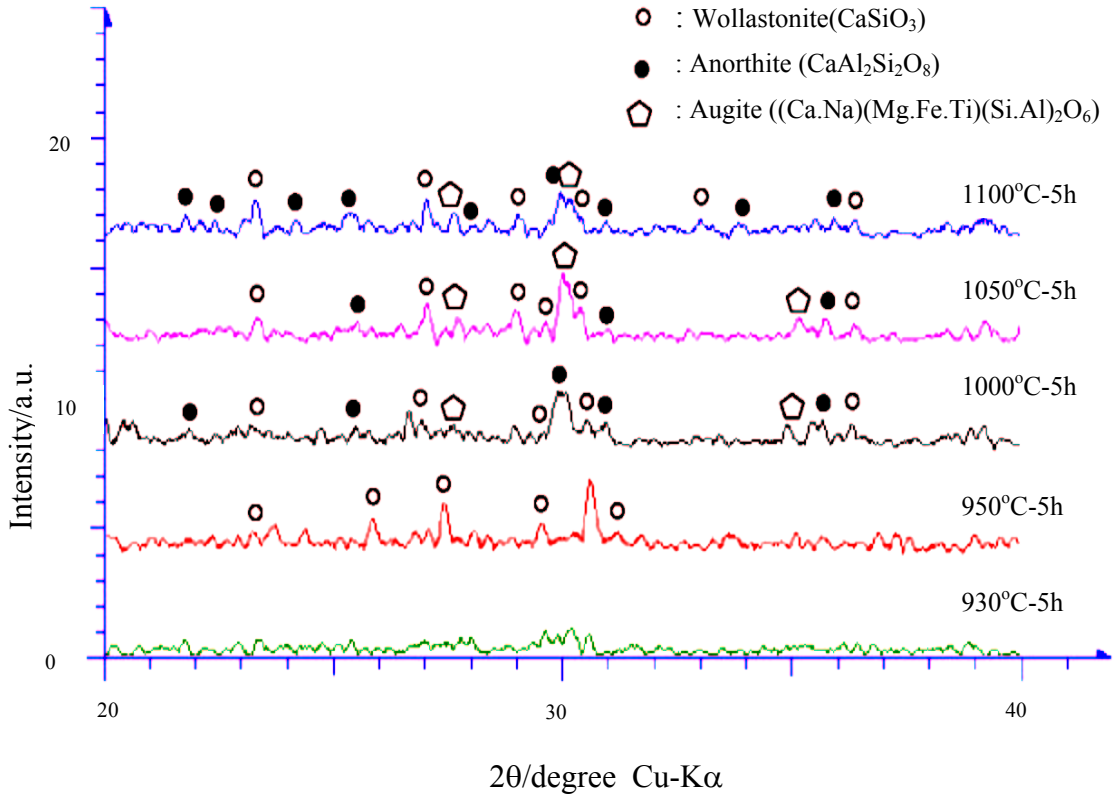

Figure 6.11(a) XRD patterns of GC-3 glass-ceramics, 1st heat treatment 750°Cfor 10h.

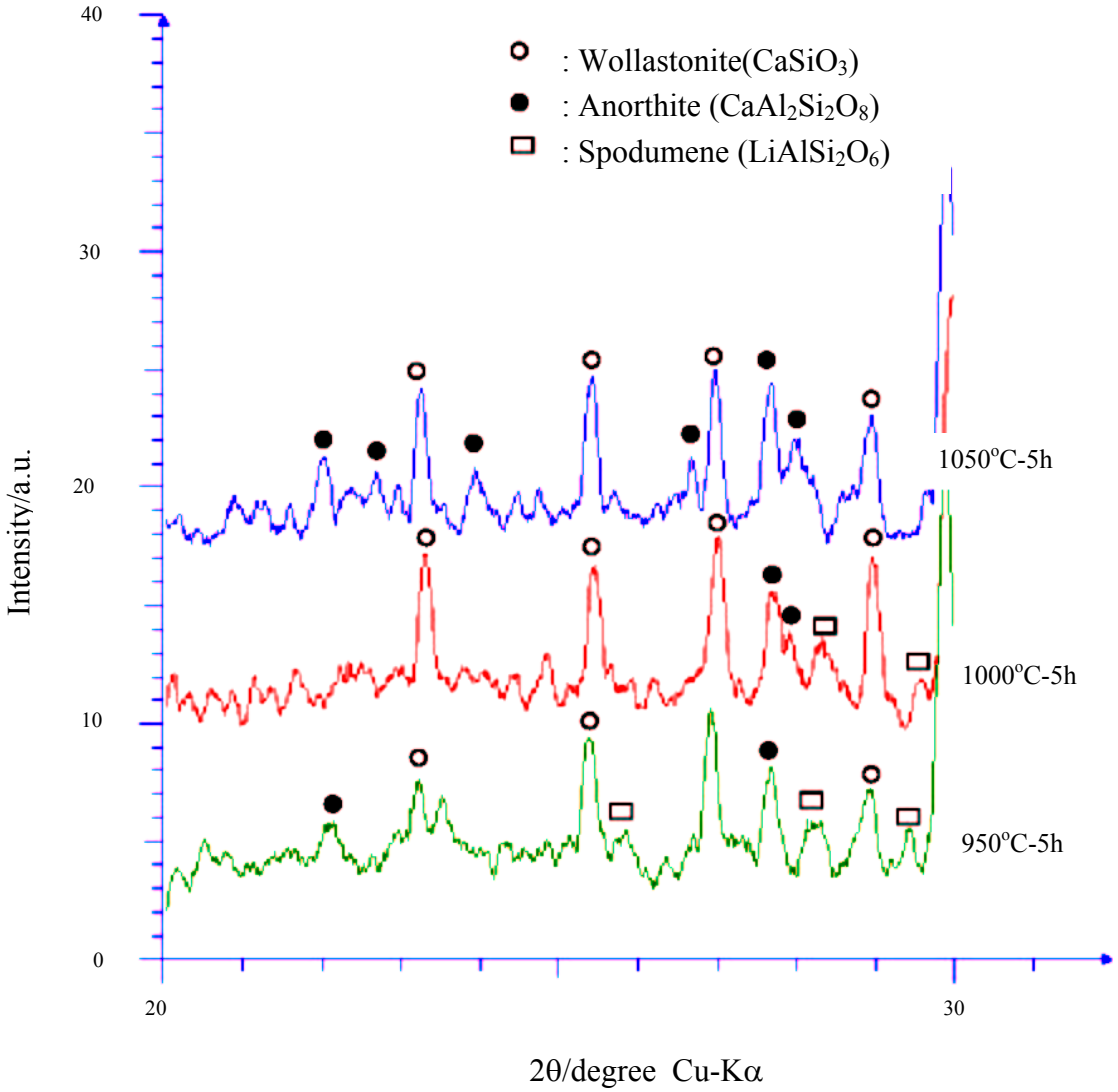

Figure 6.11(b) XRD patterns of GC-5 glass-ceramics,

1st heat treatment 750°Cfor 10h.

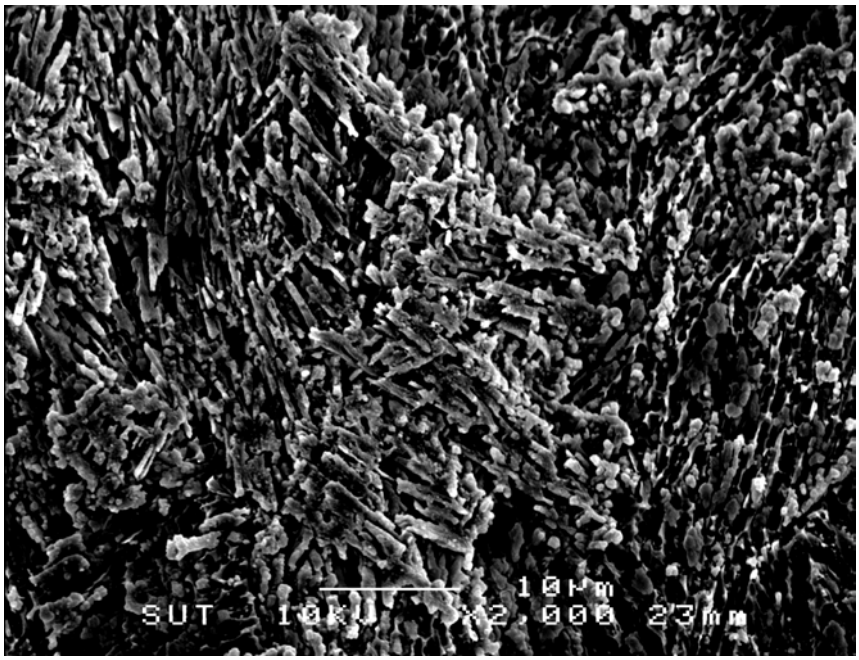

1) GC-3 750°C-10h, 950°C-10h.

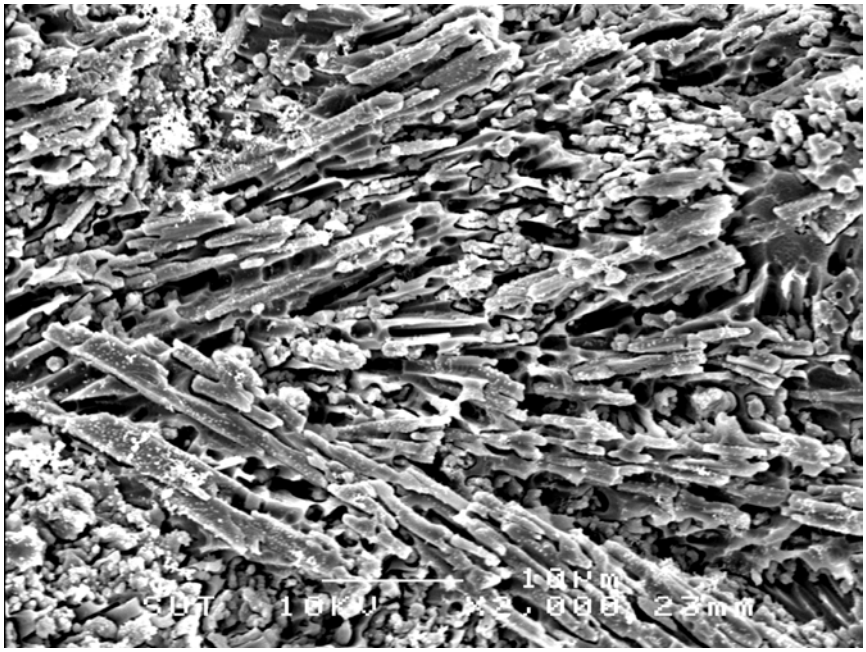

2) GC-3 750°C-10h, 1000°C-10h.

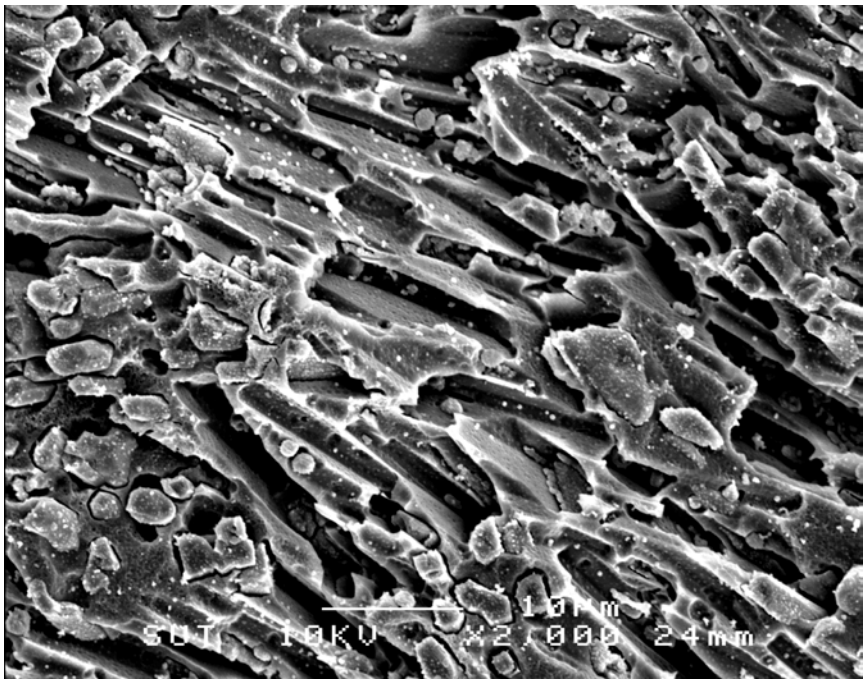

3) GC-3 750°C-10h, 1050°C-10h.

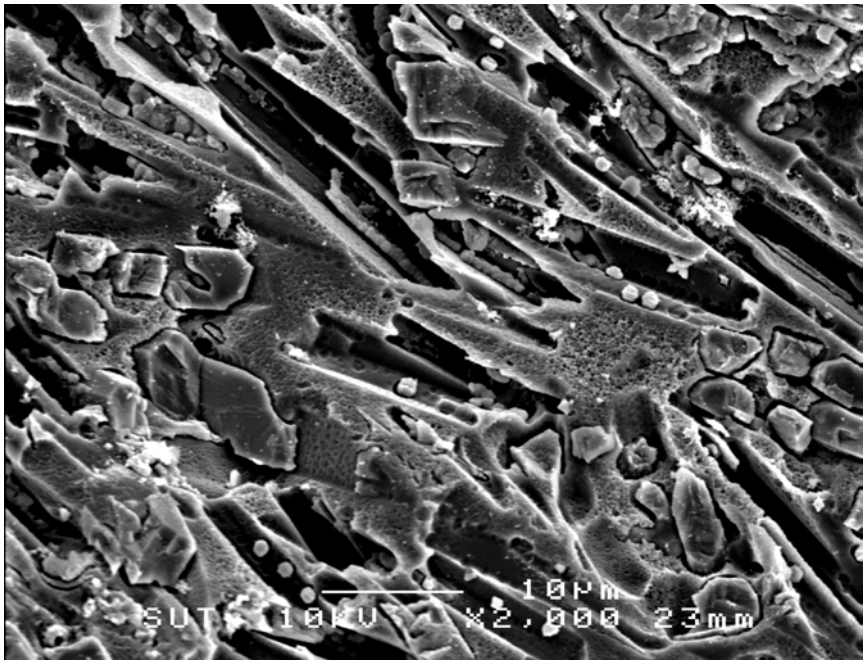

4) GC-3 750°C-10h, 1100°C-10h.

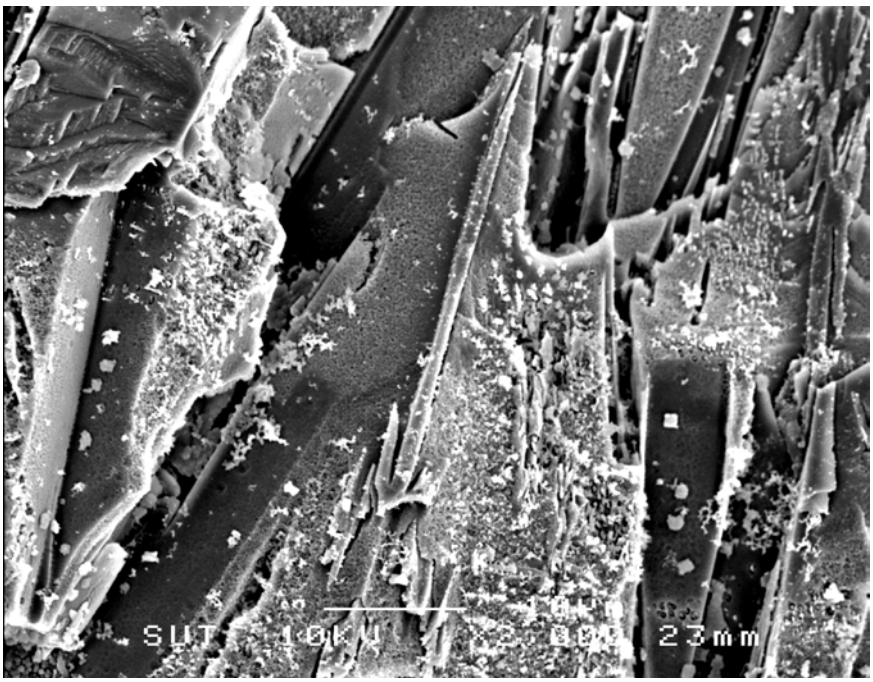

5) GC-3 750°C-10h, 1150°C-10h.

Figure 6.12 SEM photos of GC-3 glass-ceramics.

6.3 Properties of glass-ceramics

The properties of glass-ceramics are summarized in Table 6.4. It should be noticed that the heat treatment condition, 750°C-10h and 950°C-5h is not optimum one for the crystallization of each glasses. These values are one example of glass-ceramics.

Table 6.4 Properties of glass-ceramics studied.

No.	Heating Condition (^oC-hr)	Crystalline Phase[1]	α[2] ($x10^{-7}/K$)	Density (g/cm^3)	Chemical durability[3]		Fracture strength σ[4] (MPa)	Crystallization behavior
					Acid (-Δ %)	Alkali (-Δ %)		
GC-0	750-10,950-5	-	90	2.710	1.29	0.54	135.1±58.6 134.7±51.4	Surface
GC-1	750-10,950-5	W,An,Au	105	2.685	1.19	0.45	219.3±52.5 198.3±47.6	Bulk
GC-2	750-10,950-5	W,Au	100	2.674	1.09	0.37	194.9±70.8 176.5±50.5	Bulk
GC-3	750-10,950-5	W	85	2.718	1.51	0.53	206.2±43.1 193.6±37.0	Bulk
GC-4	750-10,950-5	W,Sp	85	2.696	1.86	0.53	210.4±45.7 195.6±39.5	Bulk
GC-5	750-10,950-5	W,An,Sp	85	2.657	1.67	0.32	230.4±39.6 211.4±6.7	Bulk

1 W,An,Au,Sp = Wollastonite, Anorthite, Augite, Spodumene

2 α : 100-300 ^oC

3 % change in weight(positive value = weight loss)

4 upper : non-abraded, lower : abraded (320# abrasive paper)

6.3.1 Thermal expansion

The thermal expansion coefficient of glass-ceramics does not change by crystallization, almost the same as those of glasses.

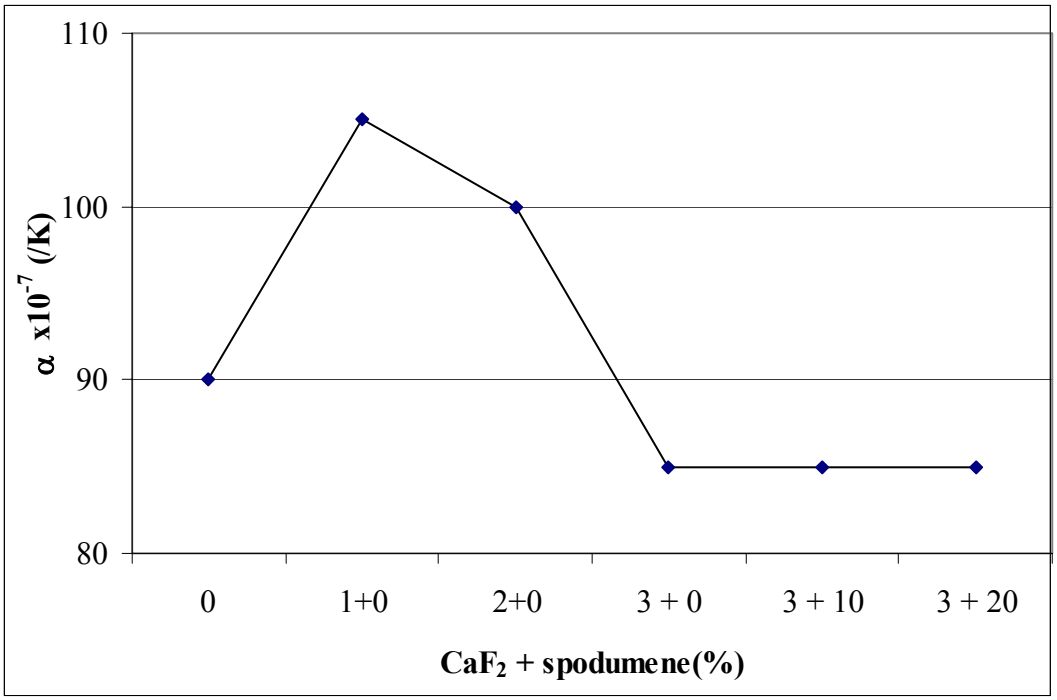

Figure 6.13 Coefficient of expansion of series I and II glass-ceramics.

(heat treatment 750°C – 10 h and 950 °C – 5h.)

6.3.2 Density

Density increases with similar tendency to those of glasses.

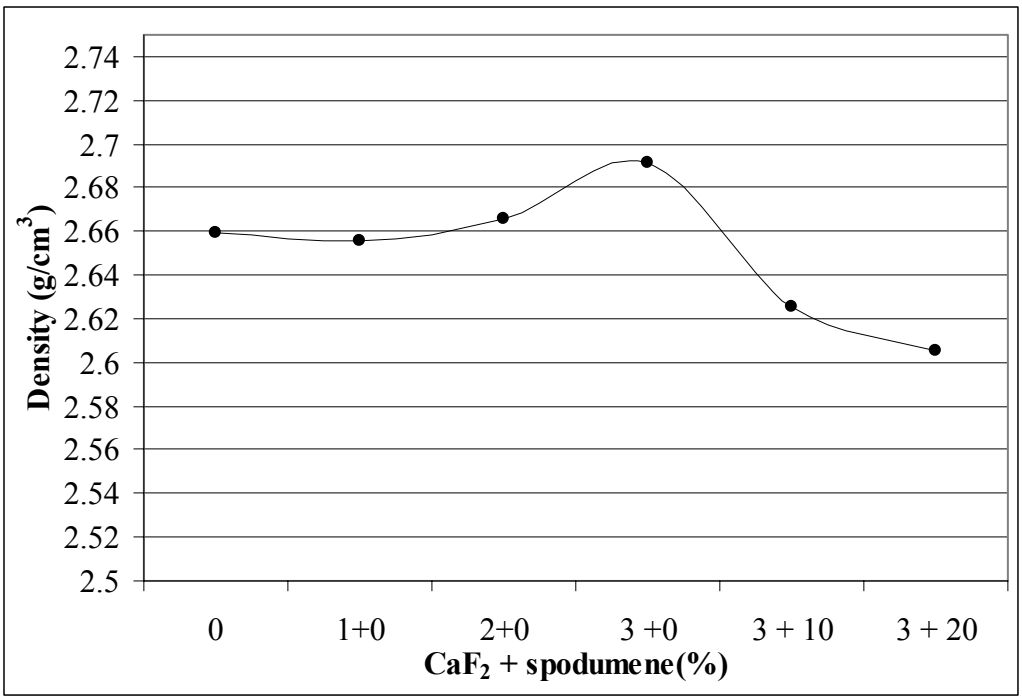

Figure 6.14 Density of series I and II glass-ceramics.

(heat treatment 750°C – 10 h and 950 °C – 5h.)

6.3.3 Chemical durability

Acid durability of series I and II glass-ceramics are improved by the crystallization of glasses.

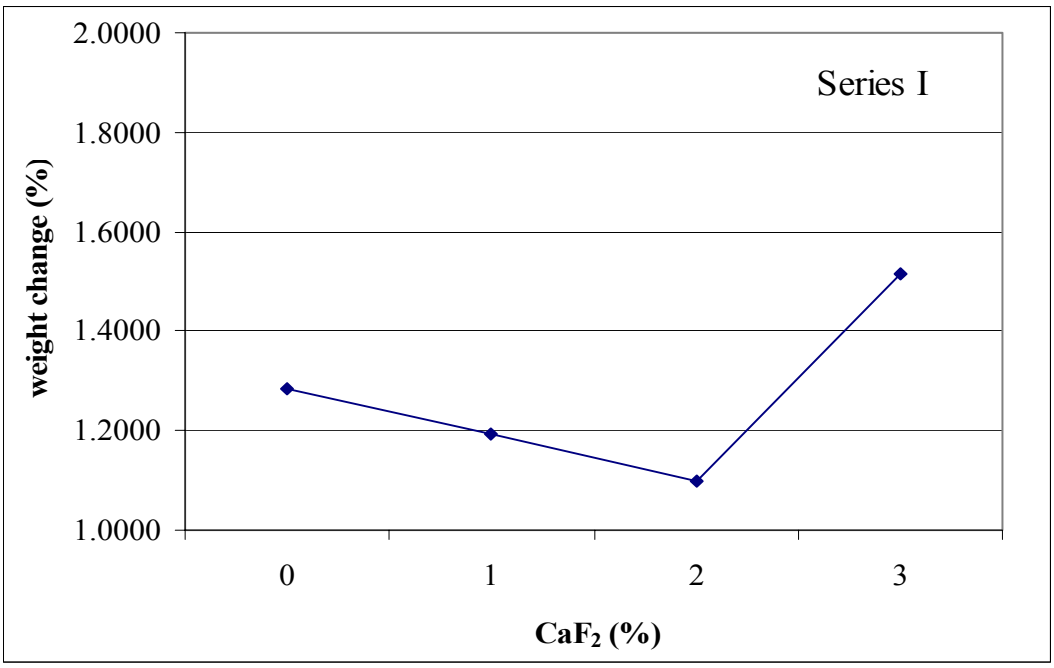

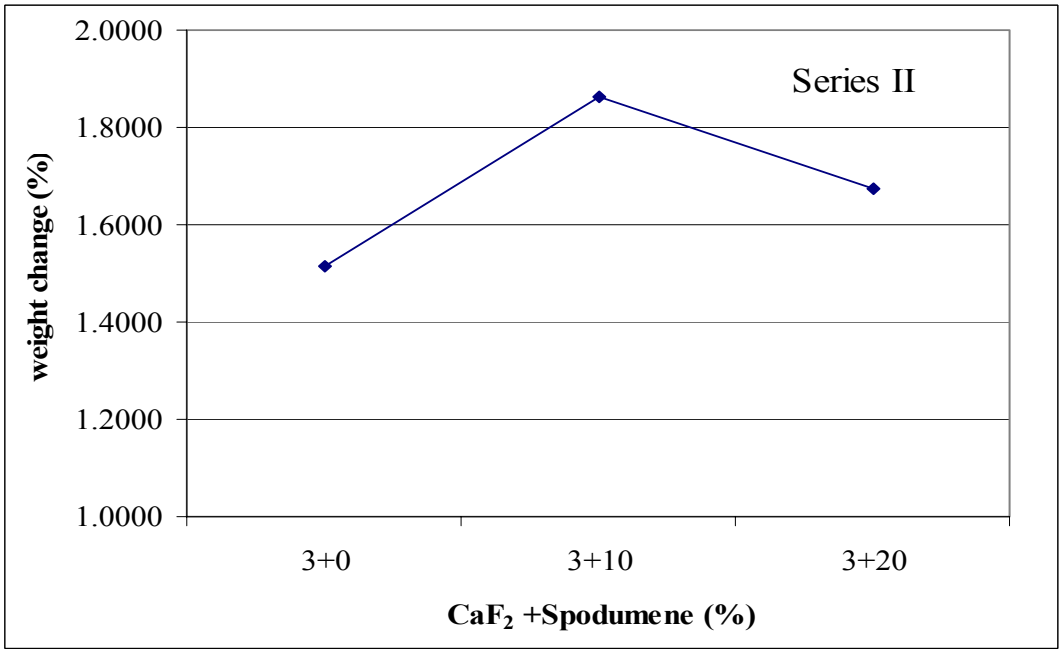

Figure 6.15 Acid durability of series I and II glass-ceramics.

(heat treatment 750°C – 10 h and 950 °C – 5h.)

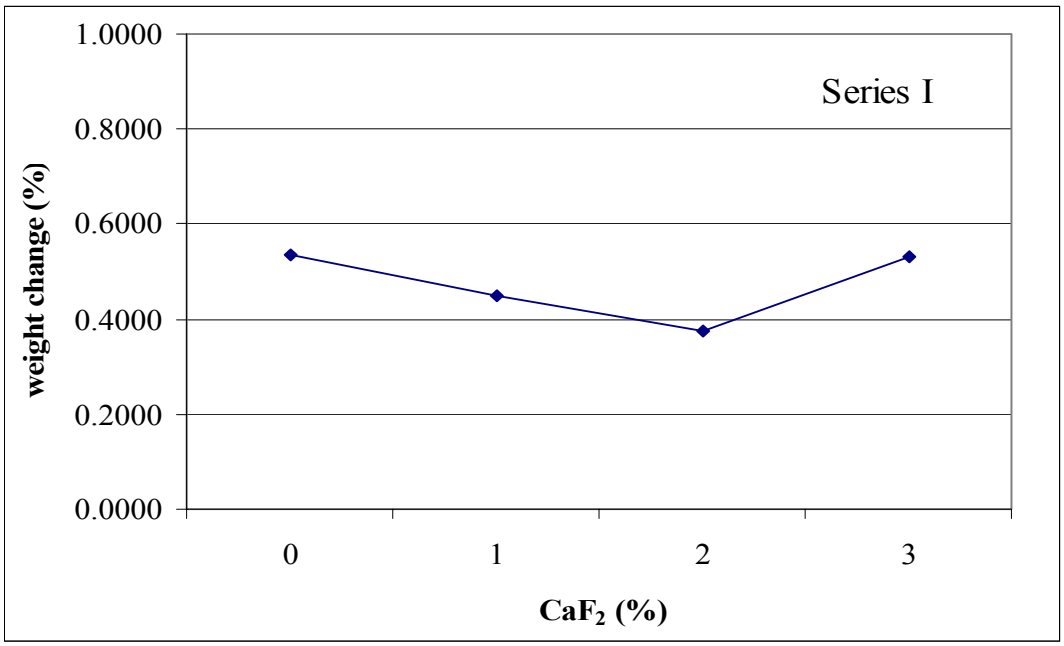

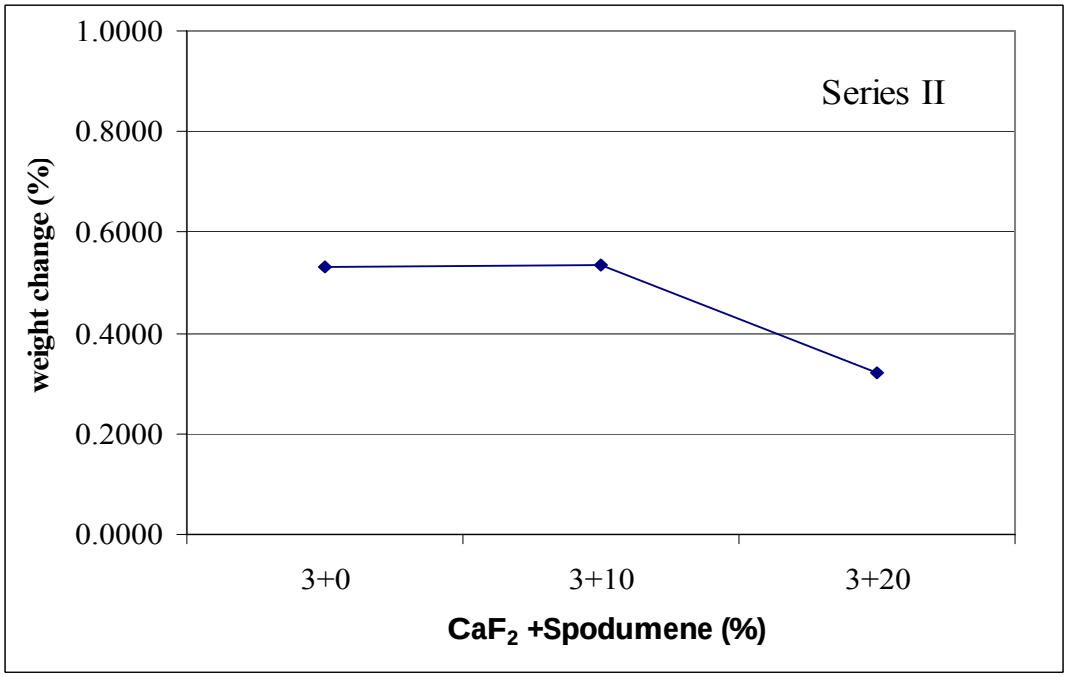

Figure 6.16 Alkaline durability of series I and II glass-ceramics.

(heat treatment 750°C – 10 h and 950 °C – 5h.)

6.3.4 Fracture strength

Fracture strength of glass-ceramics increases by 2 times comparing with those of glasses, non-abraded ~220 MPa, abraded ~ 200 MPa.

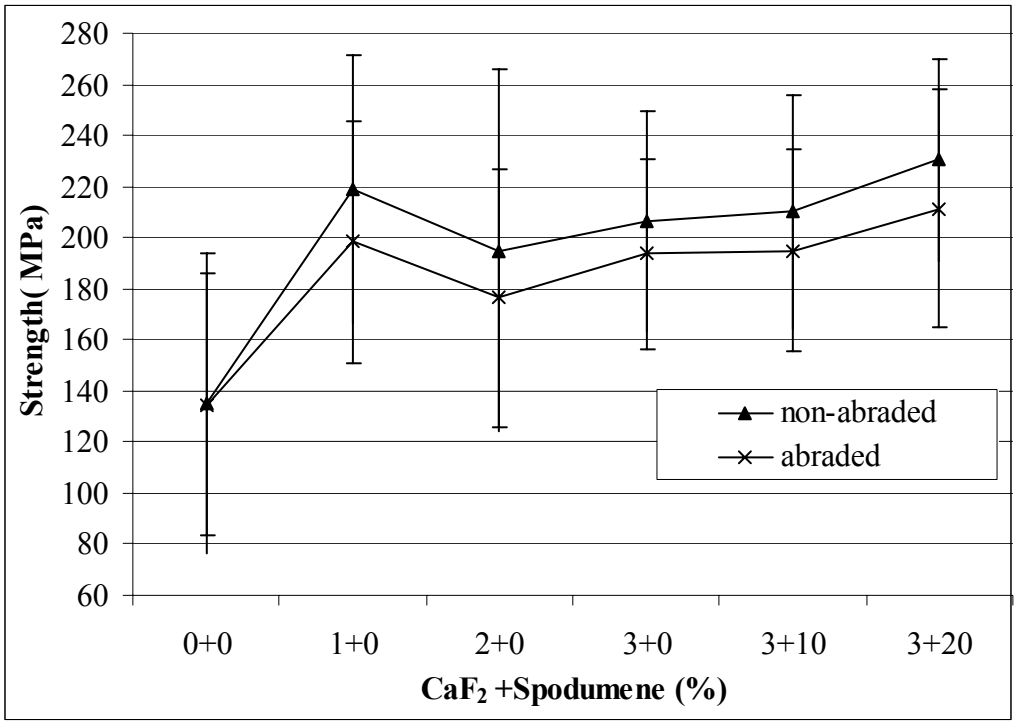

Figure 6.17 Fracture strength of series I and II glass-ceramics.

(heat treatment 750°C – 10 h and 950 °C – 5h.)

6.3.5 Thermal shock resistance.

Table 6.5 shows ΔT of glasses and glass-ceramics by calculation and experiment. And by calculation ΔT were higher than experiment because of some effect of estimation value of E and μ. No crack was observed by the water quenching at ΔT 180 °C for GC-1 to GC-5 specimens (glass-ceramics). For GC-1 to GC-5 glass-

ceramics microstructure had various crystal growth in any direction and various quantity that showed high flexural strength, which effect on high thermal shock resistance properties.

Table 6.5 Thermal shock resistance of glasses and glass-ceramics studied.

No.	Additives[1]		α^2($x10^{-7}$/K)	Fracture strength	ΔT(^oC)		Apperance
	CaF_2	Spodumene		(MPa)	Calculation	Experiment	
G-0	0	0	95	100.4	105.68	80	Crack
G-1	1	0	95	111.6	117.48	80	Crack
G-2	2	0	95	125.9	132.48	80	Crack
G-3	3	0	85	124.5	146.48	100	Crack
G-4	3	10	85	120.5	141.76	100	Crack
G-5	3	20	85	115.6	136.00	100	Crack
GC-0	0	0	90	135.1	150.09	130	Crack
GC-1	1	0	105	219.3	208.82	180	No crack
GC-2	2	0	100	194.9	194.88	180	No crack
GC-3	3	0	85	206.2	242.62	180	No crack
GC-4	3	10	85	210.4	247.53	180	No crack
GC-5	3	20	85	230.4	271.11	180	No crack

1 Additional weight%

2 α : 100-300 ^oC

3 From $\Delta T = \sigma.(1-\mu)/E.\alpha$ (For glass and glass-ceramics, E = 70 GPa and μ = 0.3)

CHAPTER VII

DISSUSIONS

7.1 Phase separation and crystallization

Generally a small amount of additives is widely used in glass-ceramics processing. This additive is called nucleating agents, which results in fine grained glass-ceramics articles without deformation of original glasses. It was considered that their roles are

(1) Promotion of phase separation and

(2) Provision of the surface for heterogeneous nucleating site.

It is well known that F acts as an optimum nucleating agent for LiO_2-Al_2O_3-SiO_2 system and Na_2O-CaO-MgO-SiO_2 system of glasses. F promotes phase separation of parent glasses, and the composition of one of which is similar to certain crystals and a certain crystal precipitate in that phase.

Although an apparent phase separation was not observed in Series I glasses, an isolated droplet like particles can be detected by SEM observation. However, the systematic change in the structure cannot be observed with CaF_2 content. On the other hand, DTA indicated that the crystallization onset and peak temperature decreased with increase in the amount of CaF_2. Also, G-0 glass (without CaF_2) showed only surface crystallization, whist G-1 to G-3 glasses(with CaF_2) appeared to be bulk crystallization. This suggests that CaF_2 affects the crystallization process. CaF_2 might

act as nucleating agent. In series I glasses, the initial crystalline phase was wollastonite.Now assuming that the lattice constant of additives is a_a and that of the main crystal is a_o, if the difference between these two values is smaller than $\pm$15%, that additives may act as an effective nucleating agent.

$$\delta = 100 \times (a_a - a_o)/ a_a \qquad (7.1)$$

Let us consider the matching of lattice parameter between β-wollastonite and CaF_2. β-wollastonite has triclinic, pseudo-hexagonal and pseudo-triclinic structure. Their lattice parameters of para-wollastonite are : monoclinic(TCPDS 27-88) (a_o = 1.5426 nm, b_o = 0.732 and c_o = 0.7066 nm.) and that of CaF_2 (cubic, JCPDS 35-0816) is a_o 0.546 nm. then, δ may be given by:

$$\delta = 100 \times (3 \times 0.546 - 1.5426)/3 \times 0.546 = 5.82 \qquad (7.2)$$

The matching of lattice parameter between them is very well, therefore, CaF_2 has a potential to act as a good nucleating agent for the crystallization of β-wollastonite. However, no diffraction peaks were detected by XRD for samples heat treated at 750°C for 10 h, so that CaF_2 may affect phase separation.

On the contrary in series II glasses containing both CaF_2 and spodumene, an interconnected type phase separation can be observed clearly. This indicates that CaF_2 promotes phase separation and bulk crystallization appeared, resulting in high hardness and high mechanical strength. Thus the original glass without any additives shows only surface crystallization. Therefore, a certain nucleating agent was required

for bulk crystallization of fly ash based Na_2O-CaO-MgO-Al_2O_3-Fe_2O_3-SiO_2 system of glasses.

7.2 Chemical durability

The ions such as alkaline or alkaline earth can be fixed in certain sites of crystals by the crystallization, and hence the ion exchange reaction of these ions and H^+ ion in acid might be eliminated, and the chemical durability of glass-ceramics is expected to be improved by the crystallization. Generally, the chemical durability of glass-ceramics is higher than that of glasses. However, if alkaline or alkaline earth ions are enriched in residual glassy matrix phases, this phase becomes weak in chemically, and consequently the higher chemically durable glass-ceramics cannot be obtained. Any, it is considered that the corrosion of glass-ceramics in acid or alkaline solution proceeds by the corrosion of residual glassy matrix phase.

From the experiment, the preparation of glass and glass-ceramics specimens was not homogeneous because of difference density and melting behavior of raw materials. Even two or three times remelted, glass and glass-ceramics still showed different color, that mean non homogeneous samples were occurred. So that the pieces of grounded specimens were not homogeneous. The chemical durability of ground specimens cannot show the accurate tendency, it depended on the sampling of specimens.

7.3 Thermal Expansion Coefficient

From the experiment, the thermal expansion coefficient of glass-ceramics did not change even added spodumene on the composition. In this study, the crystalline

phases precipitated are wollastonite, anorthite, and spodummene, among which only spodumene shows low thermal expansion coefficient, but the amount of lithium is too small. Therefore, glass-ceramics were obtained here exhibits rather high thermal expansion coefficient.

7.4 Fracture Strength

For the nucleation 750°C for 10 hour and crystallization 950°C for 5 hour, The fracture strength of glass-ceramics without CaF_2 were showed 135 MPa, which almost the same as fracture strength of glasses because of surface crystallization of glass-ceramics were occurred. Whereas the fracture strength of glass-ceramics with 3% CaF_2 were showed 210 MPa. The glass-ceramics were occured bulk crystallization and the percent crystallinity was 27.9. The three dimensional interconnected type Wollastonite crystal were precipitated and glass-ceramics with 3% CaF_2 and 20% Spodumene , the fracture strength were 230 MPa. The percent crystallinity were 53.9% and the crystal type were Wollastonite, Anorthite and spodumene were precipitated. The higher percent crystallinity of glass-ceramics would be related to higher fracture strength because of crack path would occur between glassy phase.

7.5 Thermal Shock Resistance

The thermal shock resistance of brittle materials may be expressed by the equation 1) for extreme temperature change (for example water quenching).

From this equation, the higher thermal shock resistance indicates larger ΔT. The higher thermal shock resistance can usually be achieved by lower thermal

expansion coefficient of materials. The thermal expansion coefficient of glass-ceramics is given by next equation.

$$\alpha = \{(\alpha cPcKc/\rho c) + (\alpha gPgKg/\rho g)\}/\{(PcKc/\rho c) + (PgKg/\rho g)\} \quad (7.3)$$

where ;

P ; fraction

K ; Bulk modulus

ρ ; density

α ; thermal expansion coefficient of both phases

$$\alpha = (\alpha cPcEc + \alpha gPgEg) / (PcEc + PgEg) \quad (7.4)$$

where ;

E ; Young's modulus

c ; crystal

g ; glass

If the poisson's ratio of glass and crystalline phases are almost the same, bulk modulus can be replaced by Young's modulus, and hence α of glass-ceramics may be given by equation 7.4.

It is clearly recognized that thermal expansion coefficient of glass-ceramics would be small if the thermal expansion coefficient of crystalline phases is small.

In this study, the crystalline phases precipitated are wollastonite, anorthite, augite and spodummene, among which only spodumene shows low thermal expansion

coefficient, but the amount of lithium is small. Therefore, glass-ceramics obtained here exhibits rather high thermal expansion coefficient.

On the contrary, if the fracture strength is higher, the higher thermal shock resistance can also be achieved. Usually, the fracture strength of glass-ceramics is higher than that of glasses, there is possibility to obtain high thermal shock resistance. Now assuming for GC-5,

$\alpha = 85 \times 10^{-7}$ /K ,

$\sigma = 230$ MPa ,

E = 70 GPa ,

$\mu = 0.3$

From :

$$\Delta T = \sigma . (1-\mu)/ E.\alpha$$

$$= (230 \times 10^{6} \times 0.7)/ (70 \times 10^{9} \times 85 \times 10^{-7})$$

$$\Delta T = 271K$$

This value is 2 times larger than that of glasses. In this case, higher fracture strength provides higher thermal shock resistance.

CHAPTER VIII

CONCLUSIONS

The effective utilization of fly ash from coal fired power plant as a starting material for glass-ceramics was studied. The main purposes of this research were investigated the effect of fly ash on the strength, chemical durability and thermal shock resistance of glass-ceramics.

The following results were obtained.

1 Fly ash was consist of about 75 percent of glassy phase with a small amount of α- Quartz, anorthite and gehlenite crystals and unkwon. The average particle size of fly ash was about 33 μm.

2 The composition of fly ash was

SiO_2-Al_2O_3-Fe_2O_3-MgO-CaO-Na_2O-K_2O.

3 About 35 % of fly ash can be introduced as a starting material.

4 Clear and bubble free glasses were obtained by the melting at 1450°C for 2h. Glasses appear to be brown in color because of high Fe_2O_3 content.

5 Glass transition temperature and thermal expansion coefficient of glasses were about 600°C and 90 x 10^{-7} /K, respectively.

6 Glasses containing CaF_2 exhibit bulk crystallization, but surface crystallization for glasses without CaF_2.

7 Crystalline phases precipitated by the heat treatment were β-wollastonite, anorthite and augite for glass containing CaF_2.

8 The interconnected type phase separation was observed in glasses containing both CaF_2 and spodumene, and these glasses show bulk crystallization.

9 The chemical durability was improved by the crystallization. The acid and alkaline durability of glass-ceramics is better than those of glasses.

10 Fracture strength of glass-ceramics is about 230 MPa, which is 2 times higher than that of glass.

11 The thermal expansion coefficient of glass-ceramics is rather higher, 90 x 10^{-7}/K, and therefore the thermal shock resistance of that might not be higher. The thermal shock resistance of glass-ceramics is estimated to be 200K (extreme temperature change, water quenching), which is 2 times higher than that of glass.

12 Thus, the utilization of fly ash as a starting material for glass-ceramics is possible.

REFERENCES

Arun,.K.V.(1994). **Fundamentals of inorganic glassed**. Academic press London.

Bach, Hans. (1995). **Low thermal expansion glass-ceramics**.Springer.

Barbieri, L., A.Corradi., and I Lancellotti. (2000). Bluk and sintered glass-ceramics by recycling municipal incinerator bottom ash. **Journal of the European Ceramic Society.** 20: 1637-1643.

Barbieri, L., A.M.Ferrari., I.Lancellotti., and C.Leonelli. (2000). Crystallization of (Na_2O-MgO)-CaO-Al_2O_3-SiO_2 glassy system formulated from waste products. **Journal of the American Ceramic Society**. 83(10):2515-2520.

Barbieri, L., I.Lancellotti., T.Manfredini., I.Queralt., J.M.Rincon., and M.Romero. (1999). Design, obtainment and properties of glasses and glass-ceramics from coal fly ash. **Fuel**. 78: 271-276.

Barbieri, Luisa, Isabella Lancellotti., Tiziano Manfredini., and Gian Carlo Pellacani. (2001). Nucleation and crystallization of new glasses from fly ash originating from thermal power plants. **Journal of American Ceramics Society**. 84(8): 1851-1858.

Beall, G.H., (1984). Glass-ceramics,Proceeding of a special symposium on commercial glass. **The American Ceramic Society**.October 17-19:157-173.

Beall, G.H., and D.A. Duke.(1980). **Glass-ceramic technology in Glass Science and Technology Vol. I.** Eds. D.R. Uhlmann and N.J. Kreidl, Academic Press, NewYork.403-445.

Beall, G.H.,(1989). Design of glass-ceramics. **Solid State Science**.vol 3, Nos.3 & 4: 333-354.

Benavidez, E., C.Grasselli., and N. Quaranta. (2003). Densification of ashes from a thermal power plant. **Ceramics International**. 29: 61-68.

Cheng, T.W., and Y.S. Chen. (2003). On formation of CaO-Al_2O_3-SiO_2 glass-ceramics by vitrification of incinerator fly ash.**Chemosphere**.51: 817-824.

Erol, M., A.Genc., M.L.Ovecoglu., E.Yucelen.,S.Kucukbayrak., and Y.Taptik. (2000). Characterization of a glass-ceramic produced from thermal power plant fly ashes. **Journal of the European Ceramic Society**. 20:2209-2214.

Erol,M., U.Demirler., S.Kucukbayrak., A.Ersoy., and M.L.Ovecoglu. (2003).Characterization investigations of glass-ceramics devloped from Seyitomer thermal power plant fly ash. **Journal of the European Ceramic Society**.23: 757-763.

Ferreira,C., A.Ribeiro., and L.Ottosen. (2003). Possible applications for municiple solid waste fly ash. **Journal of Hazardous Materials**. B96:201-216.

Gorokhovsky, A., and J.I.Escalante-Garcia. (2002). Inorganic wastes in the manufacture of glass and glass-ceramics: quartz-feldspar waste of ore refining, metallugical slag, limestone dust, and phosphorus slurry. **Journal of the American Ceramic Society.** 85(1): 285-287.

Jame,.K.(1991). **Introduction to glass science and technology**. The royal society of chemestry

Karamanov, A., G. Taglieri., and M.Pelino. (1999). Iron-rich sintered glass-ceramics from industrial wastes. **Journal of the American Ceramic Society**. 82(11):3012-3016.

Kastner, J.R., K.C.Das., N.D.Melear.(2002).Catalytic oxidation of gaseous reduced sulfur compounds using coal fly ash. **Journal of Hazardous Materials.**B95:81-90

Kingery, W.D., H.K.Bowen.,D.R.Uhlmann. (1991). **Introduction to ceramics**, second edition. John Wiley & Sons.

Kutuarni, S.M., and Kishore. (2002). Effects of surface treatments and size of fly ash particles on the compressive properties of epoxy based particulate composites. **Journal of Material Science**. 37 : 4321-4326.

Leroy, C., M.C.Ferro., R.C.C.Montreiro., and M.H.V.Fernandes. (2001). Production of glass-ceramics from coal ashes. **Journal of the European Ceramic Society.**21:195-202.

Locsei, B.P. (1964). Symposium on Nucleation and Crystallization in Glasses and Metals. Eds. W.B. Hillig and G.E. Rindone, **The American Ceramics Society.Inc.**71-75.

Mcmillan, P.W.(1964). **Glass-ceramics**. Academic press London and New York.

Romero, M., and J.M.Rincon. (1999). Surface and bulk crystallization of glass-ceramic in the Na_2O-CaO-ZnO-PbO-Fe_2O_3-Al_2O_3-SiO_2 system derived from a goethite waste. **Journal of the American Ceramic Society**. 82(5): 1313-1317.

Vassilev, Stanislav V., Christima G. Vassileva. (1996). Mineralogy of combustion wastes from coal-fired power stations. **Fuel Processing Technology**. 47: 261-280.

Wesche, K. (1991). **Fly ash in concrete properties and performance**. E&FN Spon, Chapman & Hall.

APPENDIX A

PERCENT CRYSTALLINITY CALCULATION METHOD

Calibration Curve of Glass

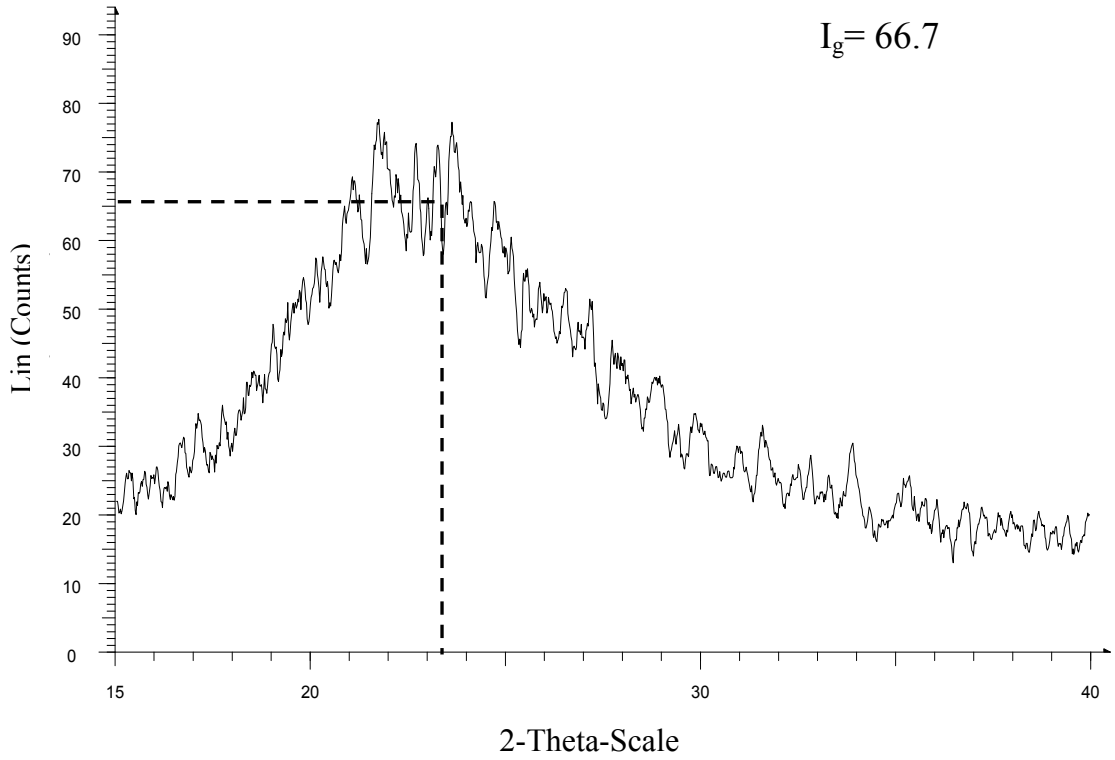

Figure 1.1A XRD pattern of 100% Glass

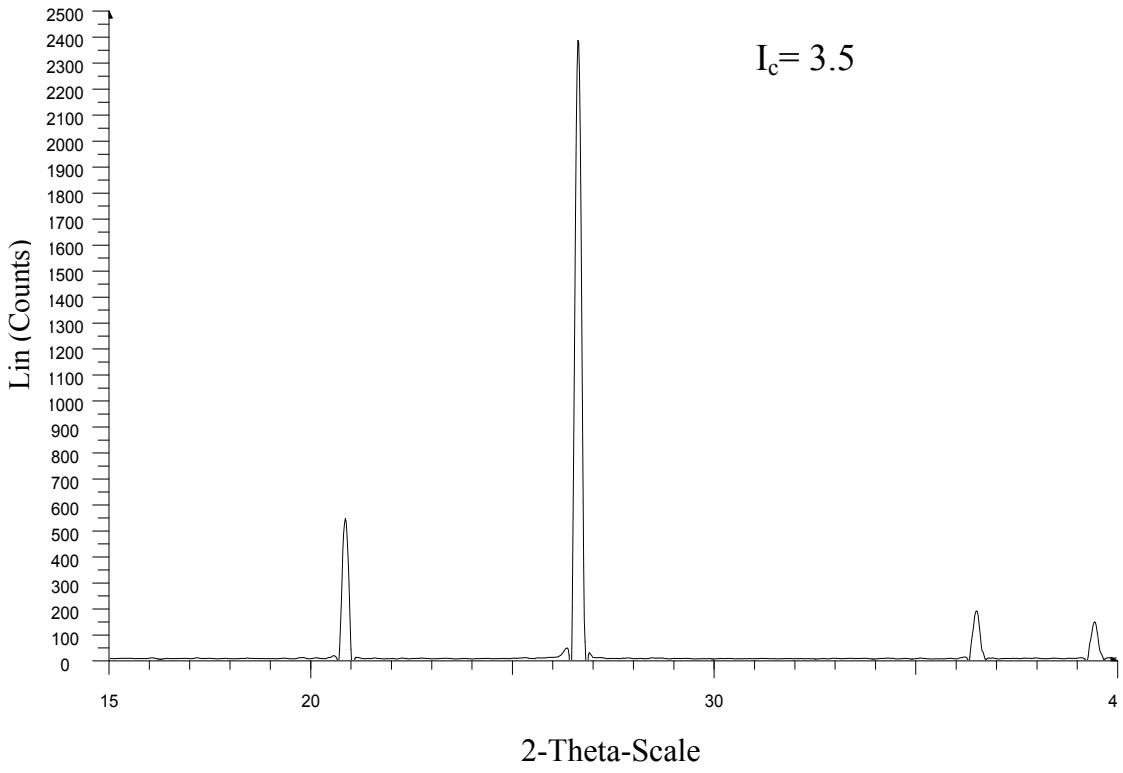

Figure 1.2A XRD pattern of 100% Quartz (crystal)

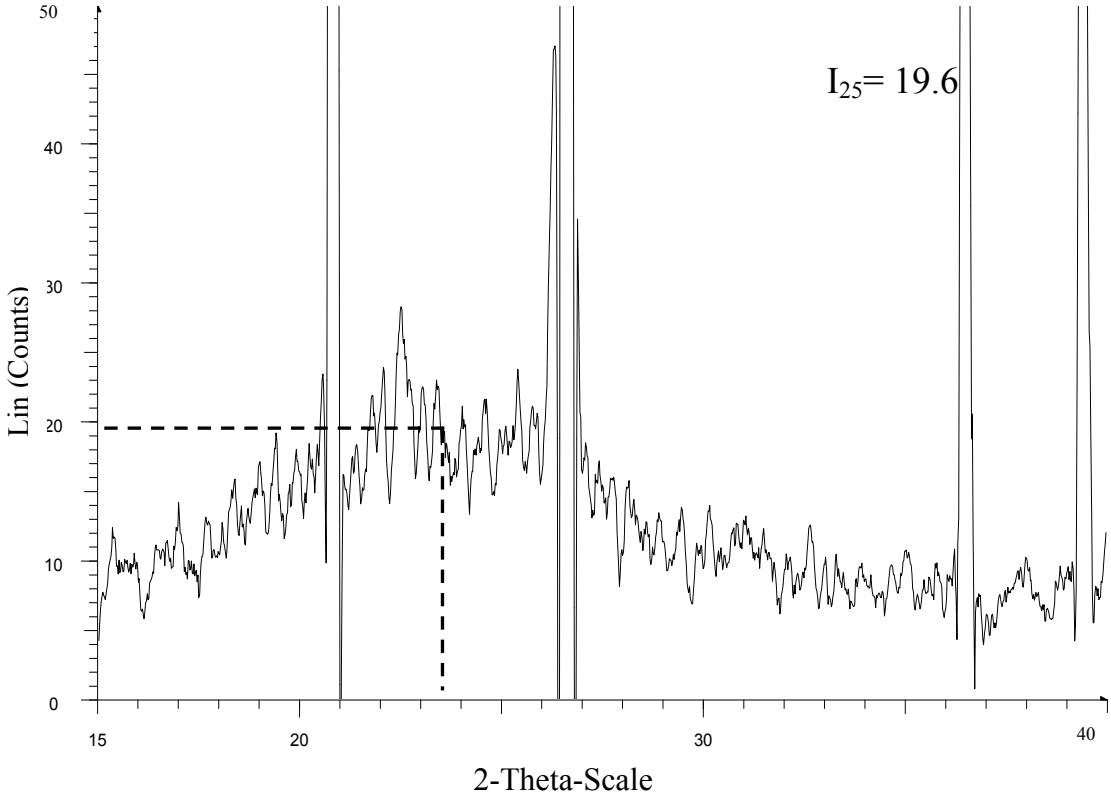

Figure 1.3A XRD pattern of 25% glass + 75% Quartz

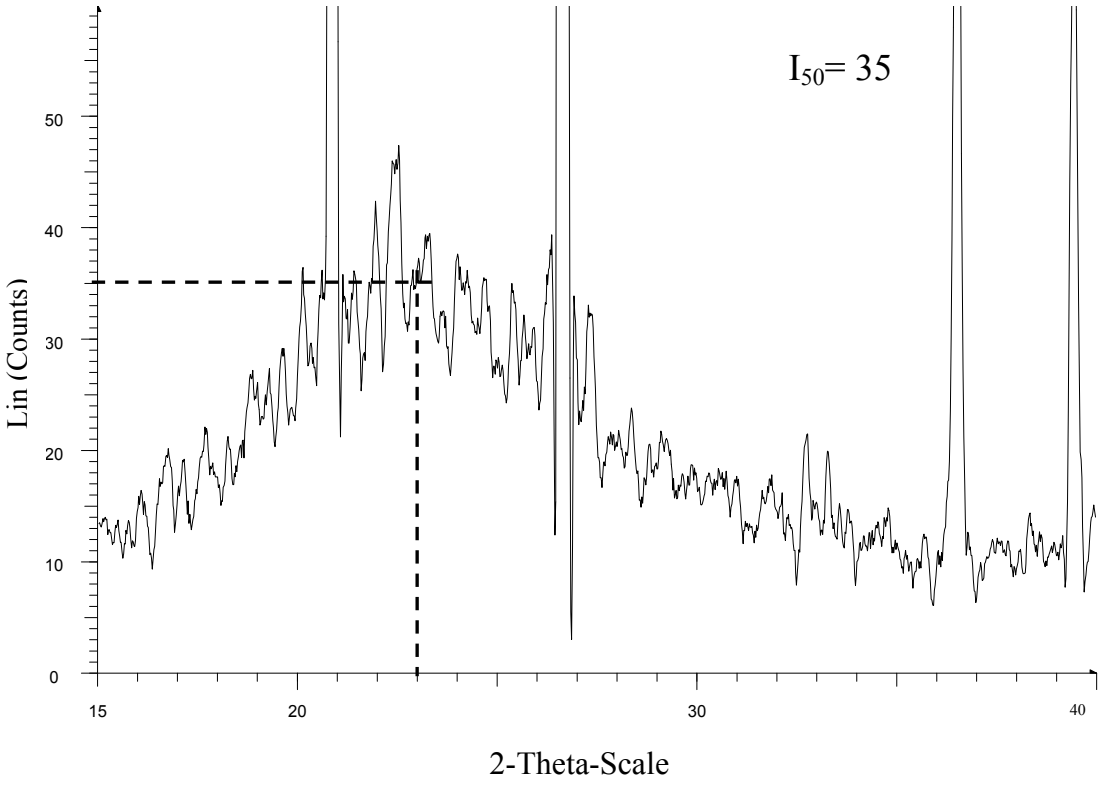

Figure 1.4A XRD pattern of 50% glass + 50% Quartz

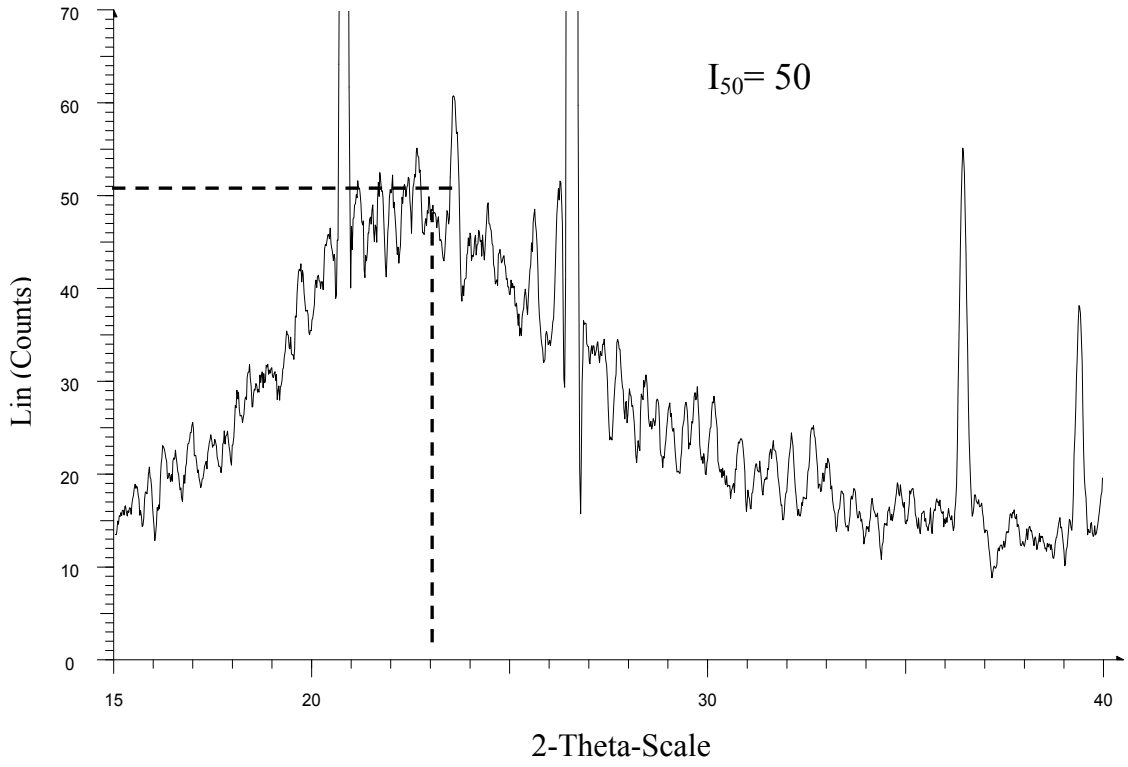

Figure 1.5A XRD pattern of 75% glass + 25% Quartz

Percent crystallinity was determined using Ohlberg and Strickler's method (Ohlberg and Strickler, 1962) and was calculated using by

$$\text{Percent crystallinity(\%C)} = \frac{(I_g - I_x)}{(I_g - I_c)} \times 100 \qquad (1.1A)$$

Where

I_g is the X-ray intensity of glass at 2θ=23°.

I_x is the X-ray background intensity of the mixtures at 2θ=23°.

I_c is the X-ray background intensity of the Quartz at 2θ=23°.

Table 1.1A The calculation of crystallinity using Ohlberg and Strickler's method.

Mixture		I_g	I_c	I_x	$\frac{I_g - I_x}{I_g - I_c} \times 100$
Glass	**Quartz**				
100	0	66.7	3.5	66.7	0
75	25	66.7	3.5	19.6	74.53
50	50	66.7	3.5	35	50.16
25	75	66.7	3.5	50	26.42
0	100	66.7	3.5	3.5	100

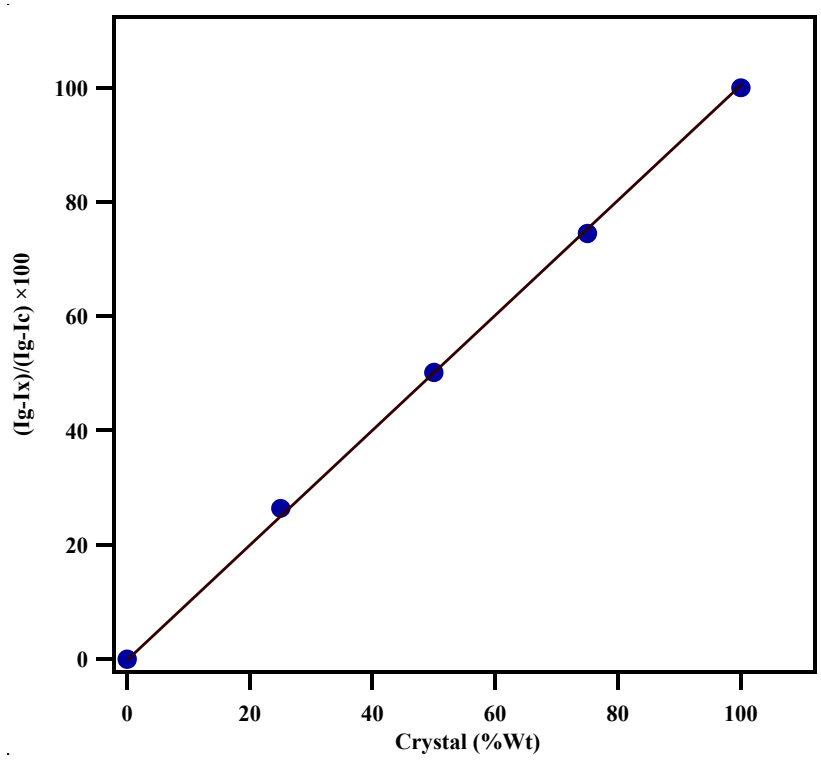

Figure 1.6A Experimentary determined crystallinity VS calculated crystallinity for mechanical mixtures of α-quartz and parent glass.

APPENDIX B

DTA CURVE DETERMINATION

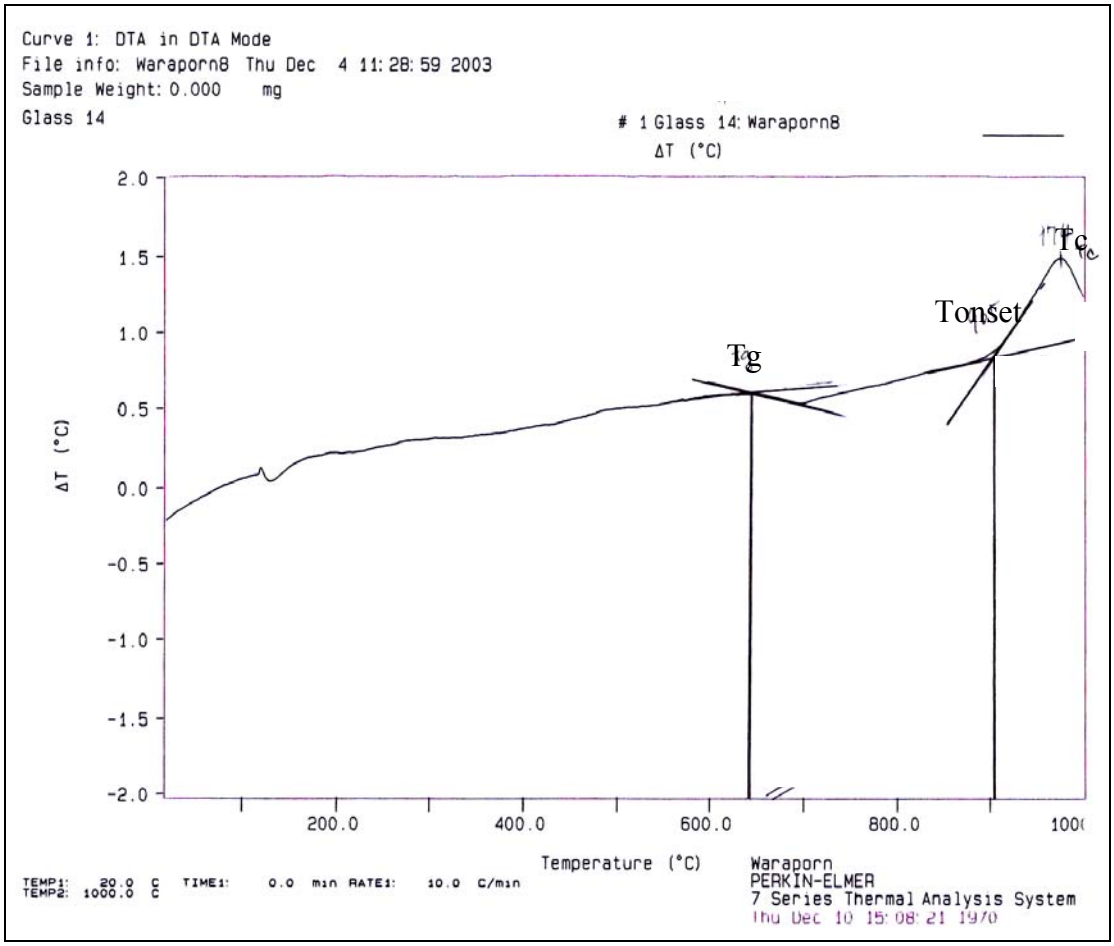

Figure 2.1A DTA curve determination

APPENDIX C

JCPDS

Table 3.1C JCPDS of SiO_2 (pattern : 01-074-0764)

Pattern : 01-074-0764 ***Radiation =*** 1.540598 ***Quality :*** Calculated

SiO_2

Silicon Oxide
Quartz, syn
Also called: Silicon oxide - HT

Lattice : Hexagonal ***Mol. weight =*** 60.08

S.G. : P6222 (180) ***Volume [CD] =*** 118.11

a = 4.99770 ***Dx =*** 2.534

c = 5.46010

Z = 3 ***I/Icor =*** 4.43

d (Å)	*i*	*h*	*k*	*l*
4.32814	207	1	0	0
3.39178	999	1	0	1
2.49885	38	1	1	0
2.30907	14	1	0	2
2.27220	1	1	1	1
2.16407	35	2	0	0
2.01181	28	2	0	1
1.84328	130	1	1	2
1.82003	1	0	0	3
1.69589	7	2	0	2
1.67773	5	1	0	3
1.63588	1	2	1	0
1.56706	59	2	1	1
1.47117	3	1	1	3
1.44271	7	3	0	0
1.40324	33	2	1	2
1.39291	55	2	0	3
1.30182	7	1	0	4
1.27555	17	3	0	2
1.24942	13	2	2	0
1.21665	15	2	1	3
1.20041	5	3	1	0
1.19794	18	1	1	4
1.17241	20	3	1	1
1.15454	1	2	0	4
1.13610	1	2	2	2
1.13059	1	3	0	3
1.09887	8	3	1	2

ICSD collection code: 026430
Temperature factor: ATF
Temperature of data collection: REM TEM 590 C.
Cancel:
Data collection flag: Non ambient temperature.

Wright, A.F., Lehmann, M.S., J. Solid State Chem., volume 36, page 371 (1981)
Calculated from ICSD using POWD-12++ (1997)

Radiation : CuKa1 ***Filter :*** Not specified

Lambda : 1.54060 ***d-sp :*** Calculated spacings

SS/FOM : F28=1000(0.0000,30)

Table 3.2C JCPDS of Gehlenite (pattern 00-004-0590)

Pattern : 00-004-0690 ***Radiation =*** 1.540560 ***Quality :*** Deleted

$Ca_2Al_2SiO_7$
$/2CaO{\cdot}Al_2O_3{\cdot}SiO_2$

Gehlenite / Calcium Aluminum Silicate

Lattice : Tetragonal

S.G. : (0)

Data collection flag: Ambient.

0PCOMC, primary reference :
Andrews.
AMMIAY, volume 34, page 717, (1949) :
Ervin, Osborn.

Radiation :

Filter : Not specified

d-sp : Not given

d (Å)	I	h	k	l
4.23140	20			
3.71014	60			
3.43913	20			
3.05900	60			
2.85038	100			
2.71979	20			
2.52996	20			
2.42942	70			
2.40941	70			
2.29983	70			
2.19037	30			
2.12008	20			
2.03984	60			
1.97018	30			
1.92030	60			
1.87032	50			
1.85005	50			
1.80999	60			
1.76021	100			
1.72029	50			
1.71023	20			
1.62992	50			
1.61006	30			
1.54975	20			
1.51985	70			
1.47021	30			
1.44991	20			
1.44023	50			
1.41976	30			
1.40998	20			
1.38989	30			
1.36990	70			
1.35989	50			

Table 3.3C JCPDS of Wollastonite (pattern 01-004-0654)

Pattern : 01-084-0654 ***Radiation =*** 1.540598 ***Quality :*** Calculated

$CaSiO_3$

Calcium Silicate
Wollastonite 1A
Also called: Calcium catena-silicate

Lattice : Anorthic (triclinic) ***Mol. weight =*** 116.16

S.G. : P-1 (2) ***Volume [CD] =*** 396.96

a = 7.92580 ***alpha =*** 90.06 ***Dx =*** 2.916

b = 7.32020 ***beta =*** 95.22

c = 7.06530 ***gamma =*** 103.43

a/b = 1.08273 ***Z =*** 6 ***I/Icor =*** 0.91

c/b = 0.96518

ICSD collection code: 201537
Temperature factor: ITF
Sample source or locality: Specimen from Willsboro, NY, USA.
Cancel:
Data collection flag: Ambient.

Ohashi, Y., Phys. Chem. Miner., volume 10, page 217 (1984)
Calculated from ICSD using POWD-12++ (1997)

Radiation : CuKa1 ***Filter :*** Not specified

Lambda : 1.54060 ***d-sp :*** Calculated spacings

SS/FOM : F30=118(0.0054,47)

d (Å)	i	h	k	l
7.67527	108	1	0	0
7.11829	1	0	1	0
7.03420	6	0	0	1
5.95783	1	-1	1	0
5.44623	17	-1	0	1
5.06139	1	0	-1	1
4.94735	25	1	0	1
*4.94735	25	0	1	1
4.70106	17	1	1	0
4.67161	34	-1	1	1
4.43051	18	1	-1	1
4.04632	84	-1	-1	1
3.83763	197	2	0	0
3.76463	46	-2	1	0
3.51710	254	0	0	2
*3.51710	254	-2	0	1
3.43529	70	-2	1	1
3.31729	339	-1	0	2
3.24351	22	2	0	1
3.20533	25	0	-2	1
*3.20533	25	-1	2	1
3.18214	53	0	-1	2
3.12505	13	0	1	2
3.10250	113	-1	1	2
3.08962	307	2	1	0
*3.08962	307	1	0	2
2.97892	999	-2	2	0
*2.97892	999	1	2	0
2.91946	72	-2	-1	1
*2.91946	72	-1	-1	2
2.79605	44	-2	2	1
*2.79605	44	-1	-2	1
2.74436	9	2	1	1
2.72312	64	1	1	2
*2.72312	64	-2	0	2
2.67899	13	-2	1	2
2.60912	14	-3	1	0
2.55842	67	3	0	0
2.53070	36	0	-2	2
*2.53070	36	-1	2	2
2.47368	157	0	2	2
*2.47368	157	2	-1	2
2.42645	1	-2	-1	2
2.37953	14	3	-1	1
2.37276	9	0	3	0
2.35383	80	-3	2	0
*2.35383	80	2	2	0
2.34473	80	0	0	3
2.33507	77	-2	2	2
*2.33507	77	3	0	1
2.30356	138	-1	3	1
*2.30356	138	-1	0	3
2.29457	80	1	-3	1
2.28156	14	-3	2	1
*2.28156	14	-2	-2	1
2.26398	2	0	-3	1
2.24226	7	0	-1	3
2.22906	3	2	1	2
2.21526	27	2	-2	2
2.21177	32	0	1	3
*2.21177	32	1	2	2
2.18586	124	1	0	3
*2.18586	124	3	-2	1
2.18234	144	2	2	1
*2.18234	144	-2	3	1
2.16784	36	-3	0	2
2.16171	22	-1	-1	3
2.13827	1	2	-3	1
2.13099	1	1	3	0
2.08986	11	-2	0	3
2.08668	12	3	1	1
2.06569	8	-1	-3	1
*2.06569	8	-2	1	3
2.04003	5	1	1	3
2.02386	59	-3	2	2
*2.02386	59	-2	-2	2
2.00668	3	-1	3	2
1.98245	39	3	0	2
1.97520	23	-1	2	3
*1.97520	23	-3	-1	2
1.94978	6	-2	-1	3
1.94654	9	0	3	2
*1.94654	9	-4	1	1
1.93863	23	-3	3	1
*1.93863	23	0	2	3
1.92255	19	2	-1	3
*1.92255	19	2	0	3
1.91882	33	4	0	0
1.89484	12	3	-2	2
*1.89484	12	-1	-2	3
1.89198	14	-2	2	3
*1.89198	14	2	2	2
1.88231	35	-4	2	0
1.87995	39	3	2	0
*1.87995	39	2	-3	2
1.86130	17	-1	-3	2
1.85573	43	-4	2	1
*1.85573	43	-3	-2	1
1.83005	199	-1	4	0
1.82490	110	-3	1	3
1.80865	20	4	0	1
1.80397	26	-2	-3	1
1.79620	39	2	-2	3
*1.79620	39	2	1	3
1.79385	38	1	2	3
1.78613	9	1	3	2
1.78312	12	4	-2	1
1.78063	15	3	2	1
*1.78063	15	0	4	0
1.77047	25	-1	4	1
*1.77047	25	-3	3	2
1.75855	85	0	0	4
1.75279	49	-4	0	2
*1.75279	49	4	1	0
1.75021	29	-1	0	4
*1.75021	29	2	3	1
1.73464	4	-2	4	1
*1.73464	4	0	-4	1
1.72363	127	-2	-2	3
*1.72363	127	-3	2	3
1.71671	101	-4	2	2
*1.71671	101	-3	-2	2
1.71174	50	-1	1	4
1.69824	20	0	1	4
*1.69824	20	-4	3	0
1.69358	12	-1	3	3
1.68769	3	-1	-1	4
1.68289	7	1	-3	3
1.67643	10	-4	3	1
1.67075	12	-2	-3	2
1.66552	6	4	1	1
1.66256	12	1	-1	4
1.65864	15	-2	0	4
*1.65864	15	-2	3	3
1.65315	7	3	0	3
*1.65315	7	-3	4	0
1.64912	7	1	4	0
*1.64912	7	0	3	3
1.64445	3	-2	1	4
1.62922	5	-4	-1	2
1.62416	23	1	-4	2
*1.62416	23	-1	4	2
1.61481	5	-1	-3	3
1.60704	49	4	-2	2
1.60487	61	3	-2	3
*1.60487	61	3	2	2
1.60211	88	0	-4	2
*1.60211	88	-2	4	2
1.58723	4	-2	-1	4
*1.58723	4	2	3	2
1.57562	13	2	-4	2
1.57351	13	0	4	2
1.56702	10	3	3	0
1.56253	13	1	-2	4
*1.56253	13	0	2	4
1.55825	8	-4	0	3
*1.55825	8	-3	3	3
1.55125	22	-1	-2	4
*1.55125	22	-2	2	4
1.54684	17	-5	2	0
*1.54684	17	2	-1	4
1.54174	7	1	3	3
1.53826	19	-5	2	1
*1.53826	19	-4	-2	1
1.53505	30	5	0	0
1.52866	24	-4	2	3
*1.52866	24	-3	-2	3
1.51880	23	-3	4	2
*1.51880	23	-1	-4	2
1.51710	18	-3	0	4
1.51459	15	4	1	2
1.50654	4	3	3	1
1.48946	13	-4	4	0
1.48745	15	2	4	0
1.48465	12	5	-2	1
*1.48465	12	4	2	1
1.47999	47	2	-2	4
1.47840	48	1	2	4
1.47366	30	2	1	4
*1.47366	30	3	-4	2
1.47131	32	5	0	1
*1.47131	32	1	4	2
1.46223	22	-5	2	2
*1.46223	22	-4	-2	2
1.45787	53	-5	0	2
1.44957	3	-2	5	0
*1.44957	3	-3	-1	4
1.44639	3	4	-1	3
1.44341	7	-5	3	1
*1.44341	7	1	-4	3
1.44189	7	-1	4	3
*1.44189	7	4	-4	1
1.43923	5	2	4	1
1.43335	21	0	-4	3
*1.43335	21	-2	4	3
1.42848	21	-1	3	4
*1.42848	21	0	-3	4
1.42112	7	4	0	3
*1.42112	7	1	-3	4

Table 3.4C JCPDS of Spodumene (pattern 00-033-0786)

Pattern : 00-033-0786 ***Radiation =*** 1.540598 ***Quality :*** High

$LiAlSi_2O_6$

Lithium Aluminum Silicate
Spodumene

Lattice : Monoclinic
S.G. : C2/c (15)

a = 9.46600
b = 8.39400 ***beta =*** 110.17
c = 5.22100
a/b = 1.12771 ***Z =*** 4
c/b = 0.62199

Mol. weight = 186.09
Volume [CD] = 389.41
Dx = 3.174
Dm = 3.123

General comments: Optical data and measured density for kunzite from Pala, San Diego Co., California, USA [Deer, W., Howie, R., Zussman, J., *Rock Forming Minerals*, **2A** 530 (1978)].
Sample source or locality: Specimen locality not known with certainty, but probably is Pala, San Diego County, California, USA.
General comments: Variety kunzite.
Optical data: A=1.660, B=1.665, Q=1.678, Sign=+, 2V=64°(calc.)
Additional pattern: To replace 00-009-0468.
Color: Pink
Data collection flag: Ambient.

Roob, C., McCarthy, G., North Dakota State University, Fargo, North Dakota, USA., ICDD Grant-in-Aid (1980)

Radiation : CuKa
Lambda : 1.54178
SS/FOM : F30= 40(0.0170,44)

Filter : Monochromator crystal
d-sp : Diffractometer

d (Å)	*i*	*h*	*k*	*l*
6.12000	40	-1	1	0
4.45000	25	2	0	0
4.36000	35	-1	1	1
4.20500	75	0	2	0
3.44400	35	1	1	1
3.19000	35	0	2	1
3.05200	6	2	2	0
2.92100	100	-2	2	1
2.86000	12	-3	1	1
2.79300	90	3	1	0
2.66900	10	1	3	0
2.55100	7	-2	0	2
2.45000	30	-1	3	1
*2.45000	30	0	0	2
2.35300	10	2	2	1
2.22300	4	4	0	0
2.17800	2	-2	2	2
2.14600	5	3	1	1
2.10700	14	1	1	2
2.05900	10	-3	3	1
2.03400	5	3	3	0
1.96300	1	4	2	0
1.92900	10	0	4	1
1.86300	18	-2	4	1
1.84600	5	-5	1	1
1.82900	5	-4	2	2
1.78700	1	-3	3	2
1.73900	5	5	1	0
*1.73900	5	3	3	1
1.71800	1	1	3	2
1.68800	1	2	4	1
1.68100	1	-1	1	3
1.66600	1	-3	1	3
1.64900	3	1	5	0
1.62000	2	-2	4	2
1.60700	10	-2	2	3
1.60200	8	3	1	2
1.59400	5	-1	5	1
*1.59400	5	0	4	2
1.56820	16	-5	3	1
1.52550	7	4	4	0
1.52240	5	0	2	3
1.49240	2	1	1	3
1.48100	2	6	0	0
1.47550	1	-6	2	1
1.45990	7	3	5	0
*1.45990	7	-4	4	2
1.39950	6	0	6	0
1.36040	4	-3	5	2
1.34570	2	0	6	1
*1.34570	2	4	2	2
1.33870	3	3	5	1
1.33020	8	5	3	1
1.31350	5	-7	1	2
1.30170	2	-2	0	4
1.28630	2	-3	1	4
1.25500	2	7	1	0
*1.25500	2	2	6	1
1.22640	3	-2	6	2
1.21510	4	-7	1	3
*1.21510	4	0	6	2
1.21310	3	-7	3	1
*1.21310	3	-5	5	2

Table 3.5C JCPDS of Anorthite (pattern 00-018-1202)

Pattern : 00-018-1202 ***Radiation =*** 1.540598 ***Quality :*** Indexed

$(Ca,Na)(Si,Al)_4O_8$

Sodium Calcium Aluminum Silicate
Anorthite, sodian, intermediate

Lattice : Anorthic (triclinic) ***Mol. weight =*** 280.42

S.G. : C-1 (0) ***Volume [CD] =*** 334.56

a = 8.17600 ***alpha =*** 93.45 ***Dx =*** 2.784

b = 12.86500 ***beta =*** 116.10 ***Dm =*** 2.720

c = 7.10200 ***gamma =*** 90.50

a/b = 0.63552 ***Z =*** 4

c/b = 0.55204

Optical data: A=1.5625, B=1.5668, Q=1.5718, Sign=+, 2V=85°
Sample source or locality: Specimen from Lake County, Oregon, USA.
General comments: Pattern obtained at 26 C using Ca F2 standard with a=5.4622, average of 3 patterns.
Analysis: Chemical analysis reports anorthite 67.2, albite 31.5, orthoclase 1.3.
Color: Colorless, light yellow
Additional pattern: See ICSD 9287 (PDF 01-071-0748); ICSD 201648 (PDF 01-086-1650); ICSD 62806 (PDF 01-078-1629).
Structure: Structural state intermediate between high and low but more similar to high.
Unit cell: Unit cell sub-cell indexes all powder reflections. True cell is a= 8.17, b=12.87, c=14.19, α=93.29, β=116.0, γ=90.77.
Data collection flag: Ambient.

Stewart, Walker, Wright, Fahey., Am. Mineral., volume 51, page 177 (1966)

Radiation : CuKa ***Filter :*** Beta

Lambda : 1.54180 ***d-sp :*** Not given

SS/FOM : F30= 34(0.0136,65)

d (Å)	*i*	*h*	*k*	*l*
6.49000	2	1	-1	0
4.68500	6	0	-2	1
4.04200	35	-2	0	1
3.90400	16	1	-1	1
3.75900	70	1	-3	0
3.63200	12	1	3	0
3.47100	20	-1	-1	2
3.42600	2	-2	-2	1
3.36500	30	-1	1	2
3.24100	40	2	-2	0
3.21000	70	0	4	0
3.20300	70	-2	0	2
3.18100	100	0	0	2
3.13200	35	2	2	0
3.02700	25	1	-3	1
2.95100	30	0	-4	1
2.93600	30	0	-2	2
2.91000	10	-2	-2	2
2.83400	30	1	3	1
2.82200	16	-2	2	2
2.65000	18	-1	3	2
2.54700	6	2	-2	1
2.51500	40	-2	-4	1
2.46500	2	2	-4	0
2.45000	4	1	-5	0
2.43900	4	2	2	1
2.41800	4	3	-1	0
2.30800	4	-3	3	1
2.28200	2	-3	-3	1
2.22800	4	1	-5	1
2.21000	2	-3	-3	2
2.15800	2	-2	2	3
2.14000	16	-1	-5	2
2.13200	35	2	-4	1
2.12600	20	0	0	3
2.10100	12	1	5	1
2.01900	2	-4	0	2
1.92700	4	-4	2	2
1.88200	6	-3	3	3
1.87900	2	-3	5	1
1.84800	2	-4	0	3
1.84400	2	-2	4	3
1.83500	10	4	0	0
1.83400	2	1	-1	3
1.81900	2	2	6	0
1.79900	10	-3	5	2
1.77200	12	-2	0	4
1.75500	2	2	-4	2
1.71600	4	0	4	3
1.71100	4	1	-7	1
1.69300	2	-4	-4	1
1.65300	6	2	4	2

BIOGRAPHY

Mrs. Waraporn Emem was born on December 25, 1968 in Chacheangsao, Thailand. She earned her Bechelor's Degree in Ceramic Science from Chulalongkorn University in 1990. She had worked in Royal Porcelain and Royal Porcelain group for 12 years and her experience was mainly in ceramic tableware industry. Afterwards, she has studied for her Master's degree in Ceramic Engineering at School of Ceramic Engineering, Institute of Engineering at Suranaree University of Technology. During her master course, she has published her research paper to SUT journal entitled 'Preparation of glass-ceramics using fly ash as a raw materials' in October 2005.In addition she presented the above topic to conference in Japan on 21 November 2005, the 46th Symposium on Glass and Photonic Materials was organized by Glass Division of the ceramic society of Japan at University of Shiga Prefecture, Hikone-City, Shiga-Prefecture, Japan.